

# Experimental Studies and Modeling of CO<sub>2</sub> Solubility in High Temperature Aqueous CaCl<sub>2</sub>, MgCl<sub>2</sub>, Na<sub>2</sub>SO<sub>4</sub>, and KCl Solutions

**Haining Zhao**

John and Willie Leone Family Dept. of Energy and Mineral Engineering, The Pennsylvania State University, University Park, PA 16802

Electrochemical Technologies Program, EMS Energy Institute, The Pennsylvania State University, University Park, PA 16802

Petroleum and Natural Gas Engineering Program, EMS Energy Institute, The Pennsylvania State University, University Park, PA 16802

**Robert M. Dilmore**

U.S. Dept. of Energy, National Energy Technology Laboratory, 626 Cochran's Mill Road, Pittsburgh, PA 15236

**Serguei N. Lvov**

John and Willie Leone Family Dept. of Energy and Mineral Engineering, The Pennsylvania State University, University Park, PA 16802

Electrochemical Technologies Program, EMS Energy Institute, The Pennsylvania State University, University Park, PA 16802

Dept. of Materials Science and Engineering, The Pennsylvania State University, University Park, PA 16802

DOI 10.1002/aic.14825

Published online April 20, 2015 in Wiley Online Library (wileyonlinelibrary.com)

*The phase equilibria of CO<sub>2</sub> and aqueous electrolyte solutions are important to various chemical-, petroleum-, and environmental-related technical applications. CO<sub>2</sub> solubility in aqueous CaCl<sub>2</sub>, MgCl<sub>2</sub>, Na<sub>2</sub>SO<sub>4</sub>, and KCl solutions at a pressure of 15 MPa, the temperatures from 323 to 423 K, and the ionic strength from 1 to 6 mol kg<sup>-1</sup> were measured. Based on the measured experimental CO<sub>2</sub> solubility, the previous developed fugacity-activity thermodynamic model for the CO<sub>2</sub>-NaCl-H<sub>2</sub>O system was extended to account for the effects of different salt species on CO<sub>2</sub> solubility in aqueous solutions at temperatures up to 523 K, pressures up to 150 MPa, and salt concentrations up to saturation. Comparisons of different models against literature data reveal a clear improvement of the proposed PSUCO<sub>2</sub> model in predicting CO<sub>2</sub> solubility in aqueous salt solutions. © 2015 American Institute of Chemical Engineers AIChE J, 61: 2286–2297, 2015*

**Keywords:** CO<sub>2</sub> solubility, aqueous solutions, activity coefficient, setschenow coefficient, PSUCO<sub>2</sub>

Additional Supporting Information may be found in the online version of this article.

**Disclaimer:** This project was funded in part by the Department of Energy, National Energy Technology Laboratory, an agency of the United States Government, through a support contract with URS Energy & Construction, Inc. Neither the United States Government nor any agency thereof, nor any of their employees, nor URS Energy & Construction, Inc., nor any of their employees, makes any warranty, expressed or implied, or assumes any legal liability or responsibility for the accuracy, completeness, or usefulness of any information, apparatus, product, or process disclosed, or represents that its use would not infringe privately owned rights. Reference herein to any specific commercial product, process, or service by trade name, trademark, manufacturer, or otherwise, does not necessarily constitute or imply its endorsement, recommendation, or favoring by the United States Government or any agency thereof. The views and opinions of authors expressed herein do not necessarily state or reflect those of the United States Government or any agency thereof.

Correspondence concerning this article should be addressed to S. N. Lvov at lvov@psu.edu.

© 2015 American Institute of Chemical Engineers

## Introduction

The phase equilibria of CO<sub>2</sub> and aqueous electrolyte solutions are important to many chemical-, petroleum-, and environmental-related technical applications, such as multi-stage flash desalination,<sup>1</sup> humidified supercritical CO<sub>2</sub> extraction,<sup>2</sup> geological CO<sub>2</sub> sequestration,<sup>3</sup> CO<sub>2</sub> enhanced geothermal system,<sup>4</sup> CO<sub>2</sub>-enhanced oil recovery,<sup>5</sup> and CO<sub>2</sub>-induced metal corrosion,<sup>6</sup> and so forth. Study of CO<sub>2</sub> solubility in single-salt aqueous solutions provides essential knowledge in understanding gas-liquid equilibrium concentration and mass-transfer rate between the CO<sub>2</sub>-rich and aqueous phases for these industrial applications.

While the solubility of CO<sub>2</sub> in single-salt aqueous NaCl solutions at elevated temperatures and pressures has been widely studied at pressures of 0.1–150 MPa and temperatures from 273 to 673 K,<sup>7–10</sup> the CO<sub>2</sub> solubility in other

**Table 1. Experimental CO<sub>2</sub> Solubility in Aqueous CaCl<sub>2</sub>, Na<sub>2</sub>SO<sub>4</sub>, MgCl<sub>2</sub>, and KCl Solutions at 323–423 K and 15 MPa**

(a) The CO <sub>2</sub> -CaCl <sub>2</sub> -H <sub>2</sub> O System			
<i>T</i> /K	<i>m</i> <sub>CaCl<sub>2</sub></sub> /mol kg <sup>-1</sup>	<i>m</i> <sub>CO<sub>2</sub></sub> /mol kg <sup>-1</sup>	$\delta m_{\text{random}}$ /mol kg <sup>-1</sup>
323	0.333	1.094	0.021
323	0.667	0.965	0.020
323	1.000	0.853	0.011
323	1.333	0.746	0.002
323	1.667	0.663	0.002
323	2.000	0.618	0.009
373	0.333	0.898	0.015
373	0.667	0.777	0.008
373	1.000	0.683	0.011
373	1.333	0.614	0.007
373	1.667	0.544	0.008
373	2.000	0.491	0.006
423	0.333	0.866	0.025
423	0.667	0.723	0.006
423	1.000	0.632	0.003
423	1.333	0.550	0.006
423	1.667	0.490	0.009
423	2.000	0.442	0.004

(b) The CO <sub>2</sub> -Na <sub>2</sub> SO <sub>4</sub> -H <sub>2</sub> O system			
<i>T</i> /K	<i>m</i> <sub>Na<sub>2</sub>SO<sub>4</sub></sub> /mol kg <sup>-1</sup>	<i>m</i> <sub>CO<sub>2</sub></sub> /mol kg <sup>-1</sup>	$\delta m_{\text{random}}$ /mol kg <sup>-1</sup>
323	0.333	1.029	0.015
323	0.667	0.866	0.022
323	1.000	0.716	0.015
323	1.333	0.584	0.016
323	1.667	0.502	0.017
323	2.000	0.442	0.015
373	0.333	0.855	0.012
373	0.667	0.729	0.010
373	1.000	0.617	0.010
373	1.333	0.534	0.013
373	1.667	0.452	0.007
373	2.000	0.395	0.012
423	0.333	0.831	0.025
423	0.667	0.710	0.026
423	1.000	0.611	0.016
423	1.333	0.524	0.019
423	1.667	0.444	0.008
423	2.000	0.389	0.009

(c) The CO <sub>2</sub> -MgCl <sub>2</sub> -H <sub>2</sub> O system			
<i>T</i> /K	<i>m</i> <sub>MgCl<sub>2</sub></sub> /mol kg <sup>-1</sup>	<i>m</i> <sub>CO<sub>2</sub></sub> /mol kg <sup>-1</sup>	$\delta m_{\text{random}}$ /mol kg <sup>-1</sup>
323	0.333	1.071	0.007
323	0.667	0.961	0.012
323	1.000	0.834	0.020
323	1.333	0.743	0.006
323	1.667	0.671	0.022
323	2.000	0.609	0.010
373	0.333	0.875	0.009
373	0.667	0.767	0.005
373	1.000	0.664	0.001
373	1.333	0.594	0.012
373	1.667	0.533	0.016
373	2.000	0.483	0.002
423	0.333	0.815	0.012
423	0.667	0.699	0.008
423	1.000	0.618	0.023
423	1.333	0.536	0.020
423	1.667	0.468	0.012
423	2.000	0.430	0.002

(d) The CO <sub>2</sub> -KCl-H <sub>2</sub> O system			
<i>T</i> /K	<i>m</i> <sub>KCl</sub> /mol kg <sup>-1</sup>	<i>m</i> <sub>CO<sub>2</sub></sub> /mol kg <sup>-1</sup>	$\delta m_{\text{random}}$ /mol kg <sup>-1</sup>
323	0.500	1.174	0.018
323	1.000	1.112	0.007

**TABLE 1. Continued**

(d) The CO <sub>2</sub> -KCl-H <sub>2</sub> O system			
<i>T</i> /K	<i>m</i> <sub>KCl</sub> /mol kg <sup>-1</sup>	<i>m</i> <sub>CO<sub>2</sub></sub> /mol kg <sup>-1</sup>	$\delta m_{\text{random}}$ /mol kg <sup>-1</sup>
323	2.000	1.005	0.014
323	3.000	0.929	0.003
323	4.000	0.880	0.014
323	4.500	0.855	0.017
373	0.500	0.941	0.011
373	1.000	0.895	0.002
373	2.000	0.805	0.015
373	3.000	0.740	0.030
373	4.000	0.683	0.017
373	4.500	0.657	0.005
423	0.500	0.881	0.008
423	1.000	0.816	0.012
423	2.000	0.724	0.020
423	3.000	0.651	0.004
423	4.000	0.593	0.014
423	4.500	0.565	0.006

Note: The instrument error  $\delta m_{\text{instr}}$  was not listed in the table and it was estimated approximately 0.7% of the measured results (detailed error estimation please see Zhao et al.<sup>10</sup>). The range of random errors are: (1) the CO<sub>2</sub>-CaCl<sub>2</sub>-H<sub>2</sub>O system, 0.3–2.9%, the average is 1.3%; (2) the CO<sub>2</sub>-Na<sub>2</sub>SO<sub>4</sub>-H<sub>2</sub>O system, 0.7–3.6%, the average is 2.4%; (3) the CO<sub>2</sub>-MgCl<sub>2</sub>-H<sub>2</sub>O system, 0.2–3.8%, the average is 1.7%; (4) the CO<sub>2</sub>-KCl-H<sub>2</sub>O system, 0.3–4.0%, the average is 1.5%. *m*<sub>CO<sub>2</sub></sub> is the molality of CO<sub>2</sub> in aqueous phase, mol/kg; and  $\delta m_{\text{random}}$  denotes random error caused by repeated measurements.

single-salt aqueous solutions [e.g., CaCl<sub>2</sub>(aq), Na<sub>2</sub>SO<sub>4</sub>(aq), MgCl<sub>2</sub>(aq), and KCl(aq)], especially for the CO<sub>2</sub>-Na<sub>2</sub>SO<sub>4</sub>-H<sub>2</sub>O and CO<sub>2</sub>-MgCl<sub>2</sub>-H<sub>2</sub>O systems, have not been fully investigated. Considering NaCl, CaCl<sub>2</sub>, MgCl<sub>2</sub>, Na<sub>2</sub>SO<sub>4</sub>, and KCl are the five most frequently encountered salt species in natural water (groundwater, seawater, and natural brines)<sup>11,12</sup> and also common salts in industrial applications, high quality experimental data are still necessary to develop a reliable CO<sub>2</sub> solubility model for these CO<sub>2</sub>-salt-H<sub>2</sub>O systems. There are some reliable models deal with CO<sub>2</sub> solubility in aqueous solutions with salt species other than NaCl. To the best of our knowledge, one of the best thermodynamic modeling works on CO<sub>2</sub> solubility in aqueous electrolyte solutions of NaCl and Na<sub>2</sub>SO<sub>4</sub> is reported by AspenTech.<sup>13</sup> Pérez-Salado Kamps et al.<sup>14</sup> developed a model to calculate CO<sub>2</sub> solubility in aqueous KCl and K<sub>2</sub>CO<sub>3</sub> solutions with excellent results. In addition, three previously published models, which are capable of calculating CO<sub>2</sub> solubility in aqueous solutions containing a wide range of different salt species (NaCl, CaCl<sub>2</sub>, MgCl<sub>2</sub>, Na<sub>2</sub>SO<sub>4</sub>, and KCl), are considered herein for model comparison: (1) OLI: OLI Studio 9.0.6 (a commercial software developed by OLI Systems);<sup>8</sup> (2) SP2010;<sup>7,15</sup> and (3) DS2006.<sup>16,17</sup>

The objectives of this study are to (1) investigate the behavior of CO<sub>2</sub> solubility in different electrolyte solutions by measuring CO<sub>2</sub> solubility in aqueous CaCl<sub>2</sub>, Na<sub>2</sub>SO<sub>4</sub>, MgCl<sub>2</sub>, and KCl solutions at the same ionic strength (up to *I* = 6 mol kg<sup>-1</sup>) at the *P*-*T* region of 15 MPa and 323–423 K; and (2) apply and extend our previously developed CO<sub>2</sub> solubility model<sup>10</sup> for the CO<sub>2</sub>-NaCl-H<sub>2</sub>O system to the single-salt aqueous solutions of CaCl<sub>2</sub>, Na<sub>2</sub>SO<sub>4</sub>, MgCl<sub>2</sub>, and KCl within the same thermodynamic framework. This article is organized as follows: we described the experimental materials, apparatus, approaches, and results in the experimentation section. In the modeling section, we presented a general approach to extend Pitzer's activity equations for calculating activity coefficient of dissolved CO<sub>2</sub> in different types of electrolyte solutions. The modeling results are presented through a detailed comparison of different CO<sub>2</sub> solubility models against all experimental data available

**Table 2. Coefficients of Eqs. 10 and 11 for Calculating  $B_{\text{CO}_2-\text{salt}}$  and  $C_{\text{CO}_2-\text{CO}_2-\text{salt}}$**

Salt Species	$a_1$	$a_2$	$a_3$	$a_4$	$a_5$
$\text{CaCl}_2^{\text{a}}$	$-2.3219 \times 10^{-1}$	$1.306910^{-1}$	$8.0693 \times 10^{-1}$	$4.9642 \times 10^{-2}$	$7.0156 \times 10^{-3}$
$\text{Na}_2\text{SO}_4^{\text{b}}$	$1.2396 \times 10^{-1}$	$1.1765 \times 10^{-1}$	$2.0199 \times 10^{-1}$	$1.4198 \times 10^{-3}$	$-1.7424 \times 10^{-3}$
$\text{MgCl}_2^{\text{c}}$	$-5.0410 \times 10^{-2}$	$2.2742 \times 10^{-2}$	$2.3521 \times 10^{-1}$	$1.1069 \times 10^{-1}$	$-2.8093 \times 10^{-4}$
$\text{KCl}^{\text{d}}$	$-1.8409 \times 10^{-1}$	$6.2729 \times 10^{-2}$	$5.0722 \times 10^{-1}$	$8.7653 \times 10^{-2}$	$-2.6025 \times 10^{-3}$

<sup>a</sup>For the  $\text{CO}_2\text{-CaCl}_2\text{-H}_2\text{O}$  system, the parameters  $a_1$  to  $a_5$  were determined from the experimental data of this study and literature.<sup>22,23-27</sup>

<sup>b</sup>For the  $\text{CO}_2\text{-Na}_2\text{SO}_4\text{-H}_2\text{O}$  system, the parameters  $a_1$  to  $a_5$  were determined from the experimental data of this study and literature.<sup>23,26,28-30</sup>

<sup>c</sup>For the  $\text{CO}_2\text{-MgCl}_2\text{-H}_2\text{O}$  system, the parameters  $a_1$  to  $a_5$  were determined from the experimental data of this work and Yasunishi and Yoshida.<sup>26</sup>

<sup>d</sup>For the  $\text{CO}_2\text{-KCl-H}_2\text{O}$  system, the parameters  $a_1$  to  $a_5$  were determined from the experimental data of this and other studies.<sup>14,26,31,32,27,33,34</sup>

to us; finally, we interpreted and discussed the different behaviors of  $\text{CO}_2$  solubility in various electrolyte solutions. In the end of this study, we proposed an approach to further extend the  $\text{CO}_2$  solubility model for predicting  $\text{CO}_2$  solubility in natural or synthetic brines (mixed-salt aqueous system).

## Experimentation

The carbon dioxide used in all experiments was Coleman Instrument grade with a purity of 99.99%. Water was purified by a Milli-Q system and was degassed before being loaded into the autoclave. The purified water conductivity was below  $6 \times 10^{-6} \text{ S m}^{-1}$ . All aqueous salt solutions were prepared using this Milli-Q water and ACS Grade reagents: calcium chloride ( $\text{CaCl}_2 \cdot 2\text{H}_2\text{O}$ , AlfaAesar, 99%), sodium sulfate ( $\text{Na}_2\text{SO}_4$ , Amresco, 99%), magnesium chloride ( $\text{MgCl}_2$ , Alfa Aesar, 99%), and potassium chloride (Alfa Aesar, 99%).

The experimental system consisted of a 600-mL stainless steel autoclave (Parr Instrument Co.), a 40-mL stainless steel sample cell, a liquid  $\text{CO}_2$  pump, and a 300-mL stainless steel pressure cell for sample analysis. Details on the  $\text{CO}_2$  solubility measuring technique and the error analysis approach can be found in Zhao et al.<sup>10</sup> The experimental  $\text{CO}_2$  solubility results at a pressure of 15 MPa and temperatures from 323 to 423 K in aqueous  $\text{CaCl}_2$ ,  $\text{Na}_2\text{SO}_4$ ,  $\text{MgCl}_2$ , and  $\text{KCl}$  solutions at the ionic strength up to 6 mol  $\text{kg}^{-1}$  are listed in Table 1.

## Modeling

We use a fugacity-activity procedure<sup>18</sup> to calculate fluid phase equilibria for  $\text{CO}_2\text{-salt-H}_2\text{O}$  systems. The fugacity coefficients ( $\phi_{\text{CO}_2}$  and  $\phi_{\text{H}_2\text{O}}$ ) of all components in the  $\text{CO}_2$ -rich phase are calculated by a modified Redlich-Kwong equation of state (EoS),<sup>7,15</sup> and the activity coefficients for all components in the aqueous phase are calculated using the Pitzer activity model. The Pitzer activity model is selected due to its high accuracy among existed activity models for

aqueous electrolyte solutions.<sup>19</sup> The Pitzer activity model is incorporated into vapor-liquid equilibrium relationship for water and  $\text{CO}_2$  as shown by Eqs. 1–4.<sup>7,10,15</sup>

$$\phi_{\text{CO}_2} y_{\text{CO}_2} P = k_{\text{H},\text{CO}_2}^0 \exp\left(\frac{\bar{v}_{\text{CO}_2}(P - P_w^s)}{RT}\right) a_{\text{CO}_2} \quad (1)$$

$$\phi_{\text{H}_2\text{O}} y_{\text{H}_2\text{O}} P = P_w^s \phi_w^s \exp\left(\frac{\bar{v}_w(P - P_w^s)}{RT}\right) a_{\text{H}_2\text{O}} \quad (2)$$

where  $y_{\text{CO}_2}$  and  $y_{\text{H}_2\text{O}}$  are, respectively, the mole fraction of  $\text{CO}_2$  and  $\text{H}_2\text{O}$  in the  $\text{CO}_2$ -rich phase. In Eqs. 1 and 2,  $k_{\text{H},\text{CO}_2}^0$  is Henry's constant (molality scale) of carbon dioxide in pure water;<sup>10</sup> The vapor pressure ( $P_w^s$ ) and the fugacity coefficient of water ( $\phi_w^s$ ) were calculated using the IAPWS-95 EoS;<sup>20</sup>  $\bar{v}_{\text{CO}_2}$  is a model parameter determined by fitting model calculated results to reliable experimental data for the binary  $\text{CO}_2\text{-H}_2\text{O}$  system;<sup>10</sup> and the partial molar volume of water  $\bar{v}_w$ , was approximated by the molar volume of saturated liquid water,  $v_w^s$ , which was also calculated using the IAPWS-95 EoS. The activity of dissolved  $\text{CO}_2$  ( $a_{\text{CO}_2}$ ) and the activity of water ( $a_{\text{H}_2\text{O}}$ ) in the aqueous phase can be calculated as follows

$$a_{\text{CO}_2} = \gamma_{\text{CO}_2} m_{\text{CO}_2} \quad (3)$$

$$\ln(a_{\text{H}_2\text{O}}) = -\frac{\phi}{\Omega} [(v^+ + v^-) m_{\text{salt}} + m_{\text{CO}_2}] \quad (4)$$

where  $v^+$  and  $v^-$  are stoichiometric coefficient for cation and anion, respectively;  $m_{\text{CO}_2}$  and  $m_{\text{salt}}$  are molality of dissolved  $\text{CO}_2$  and single-salt species;  $\gamma_{\text{CO}_2}$  and  $\phi$  are the activity coefficient of dissolved  $\text{CO}_2$  and osmotic coefficient of water, which are both calculated by Pitzer equations [Appendix, Eqs. A1 and A2]; and  $\Omega$  is the number of moles of solvent in a kilogram (55.51 for water). By substituting Eq. 3 into Eq. 1 and Eq. 4 into Eq. 2, and assuming the salt species is no volatile (means  $y_{\text{H}_2\text{O}} + y_{\text{CO}_2} = 1$ ), Eqs. 1 and 2 can

**Table 3. Pitzer Triple-Ion Interaction Parameter ( $\xi_{\text{nea}}$ ) at 15 MPa**

Salt Species	$T/\text{K}$	Ionic Strength ( $\text{mol kg}^{-1}$ )							
		0.5	1	2	3	4	4.5	5	6
$\text{CaCl}_2$	323	–	0.77073	0.39436	0.26277	0.19510	–	0.15454	0.12769
	373	–	0.92645	0.46400	0.30811	0.22918	–	0.18232	0.15141
	423	–	1.10394	0.55441	0.36504	0.26831	–	0.21085	0.17319
$\text{Na}_2\text{SO}_4$	323	–	–0.05670	–0.03783	–0.03180	–0.02852	–	–0.02644	–0.02508
	373	–	–0.10374	–0.05646	–0.04081	–0.03287	–	–0.02802	–0.02489
	423	–	–0.06269	–0.04135	–0.03205	–0.02657	–	–0.02293	–0.02038
$\text{MgCl}_2$	323	–	0.63298	0.32062	0.21067	0.15474	–	0.12163	0.09991
	373	–	0.64031	0.32867	0.21797	0.16100	–	0.12696	0.10452
	423	–	0.86806	0.40224	0.25688	0.18685	–	0.14620	0.11964
$\text{KCl}$	323	0.59800	0.32006	0.16333	0.10802	0.07958	0.07004	–	–
	373	0.71435	0.36749	0.18537	0.12400	0.09210	0.08128	–	–
	423	0.95168	0.45440	0.21731	0.14267	0.10498	0.09233	–	–

**Table 4. Comparison of the Model Calculations to Experimental CO<sub>2</sub> Solubility in Various CO<sub>2</sub>-salt-H<sub>2</sub>O Systems**

Year	References	Systems	<i>P</i> /MPa	<i>T</i> /K	<i>m</i> <sub>salt</sub> /mol kg <sup>−1</sup>	<i>N</i>	Model Calculations, AAD %			
							PSUCO2	OLI <sup>d</sup>	SP2010	DS2006
1892 <sup>a</sup>	Setschenow <sup>35</sup>	CO <sub>2</sub> -CaCl <sub>2</sub> -H <sub>2</sub> O	0.1	288.4	0.1–5.0	11	4.11(11)	5.58(9) <sup>b</sup>	4.34(9) <sup>b</sup>	7.08(10) <sup>c</sup>
		CO <sub>2</sub> -KCl-H <sub>2</sub> O			1–4.3	3	1.92(3)	4.60(3)	21.47(3)	15.98(3)
1904 <sup>a</sup>	Geffcken <sup>36</sup>	CO <sub>2</sub> -KCl-H <sub>2</sub> O	0.1	288–298	0.4–1.1	8	0.70(8)	2.29(8)	10.30(8)	6.37(8)
1912	Findley and Shen <sup>37</sup>	CO <sub>2</sub> -KCl-H <sub>2</sub> O	0.1	298	0.2–1	4	0.56(4)	3.40(4)	8.25(4)	6.18(4)
1935	Kobe and Williams <sup>38</sup>	CO <sub>2</sub> -Na <sub>2</sub> SO <sub>4</sub> -H <sub>2</sub> O	0.1	298	1.76	2	1.30(2)	26.82(2)	N/A(0)	N/A(0)
		CO <sub>2</sub> -MgCl <sub>2</sub> -H <sub>2</sub> O	0.1	298	4.5	1	5.50(1)	N/A(1) <sup>b</sup>	N/A(0) <sup>b</sup>	N/A(0) <sup>c</sup>
1941	Markham and Kobe <sup>31</sup>	CO <sub>2</sub> -Na <sub>2</sub> SO <sub>4</sub> -H <sub>2</sub> O	0.1	298–313	0.2–1.5	8	0.61(8)	7.85(8)	7.03(4)	25.89(8)
		CO <sub>2</sub> -KCl-H <sub>2</sub> O		273.4–313	0.1–4	16	0.84(16)	4.59(16)	15.65(10)	10.62(16)
1945	Prutton and Savage <sup>22</sup>	CO <sub>2</sub> -CaCl <sub>2</sub> -H <sub>2</sub> O	1.5–71.2	348–394	1–3.9	116	5.58(116)	3.86(116)	9.06(104)	9.22(116)
1969 <sup>a</sup>	Gerecke <sup>32</sup>	CO <sub>2</sub> -KCl-H <sub>2</sub> O	1.5–6	274.16	0.5–3.4	40	3.69(40)	7.19(40)	16.73(40)	13.01(40)
1970	Onda et al. <sup>23</sup>	CO <sub>2</sub> -CaCl <sub>2</sub> -H <sub>2</sub> O	0.1	298	0.2–2.3	8	0.49(8)	5.94(8)	4.16(8)	1.00(8)
		CO <sub>2</sub> -Na <sub>2</sub> SO <sub>4</sub> -H <sub>2</sub> O	0.1	298	0.5–1.5	3	1.77(3)	10.60(3)	26.49(3)	30.33(3)
1972 1975	Malinin and Savelyeva <sup>24</sup>	CO <sub>2</sub> -CaCl <sub>2</sub> -H <sub>2</sub> O	4.8	298–423	0.2–6.9	25	4.32(25)	5.74(25)	1.64(25)	3.17(21) <sup>c</sup>
	Malinin and Kurovskaya <sup>25</sup>									
1979	Yasunishi and Yoshida <sup>26</sup>	CO <sub>2</sub> -CaCl <sub>2</sub> -H <sub>2</sub> O	0.1	298–308	0.2–5.3	16	3.46(16)	6.14(16)	5.76(14) <sup>b</sup>	3.16(15) <sup>c</sup>
		CO <sub>2</sub> -Na <sub>2</sub> SO <sub>4</sub> -H <sub>2</sub> O		288–308	0.2–2.4	26	3.46(26)	11.95(26)	5.35(7)	28.49(25)
		CO <sub>2</sub> -MgCl <sub>2</sub> -H <sub>2</sub> O		288–308	0.1–4.4	29	3.66(29)	9.72(29)	7.47(25)	2.63(29)
		CO <sub>2</sub> -KCl-H <sub>2</sub> O		298–308	0.4–4.8	16	0.95(16)	8.01(16)	22.39(16)	17.05(14) <sup>c</sup>
1982	Burmakina et al. <sup>33</sup>	CO <sub>2</sub> -KCl-H <sub>2</sub> O	0.1	298	0.001–0.2	8	1.15(8)	4.48(8)	5.90(8)	3.93(8)
1990	Corti et al. <sup>28</sup>	CO <sub>2</sub> -Na <sub>2</sub> SO <sub>4</sub> -H <sub>2</sub> O	1.6–20	323–348	1–3.3	24	13.91(24)	20.50(15) <sup>b</sup>	N/A(0)	38.87(8)
1993	Rumpf and Maurer <sup>29</sup>	CO <sub>2</sub> -Na <sub>2</sub> SO <sub>4</sub> -H <sub>2</sub> O	0.4–9.7	313–433	1–2	102	2.73(102)	6.91(102)	N/A(0)	27.57(102)
2002	Kiepe et al. <sup>34</sup>	CO <sub>2</sub> -KCl-H <sub>2</sub> O	0.1–10.5	313–353	0.5–4	88	10.16(88)	9.42(88)	13.58(87)	13.07(88)
2005	Bermejo et al. <sup>30</sup>	CO <sub>2</sub> -Na <sub>2</sub> SO <sub>4</sub> -H <sub>2</sub> O	2–13.1	287–369	0.25–1	113	6.70(113)	12.77(113)	12.73(24)	22.72(113)
2007	Pérez-Salado	CO <sub>2</sub> -KCl-H <sub>2</sub> O	0.4–9.4	313–433	2–4	98	1.65(98)	2.67(98)	18.35(98)	18.34(98)
	Kamps et al. <sup>14</sup>									
2011	Liu et al. <sup>27</sup>	CO <sub>2</sub> -CaCl <sub>2</sub> -H <sub>2</sub> O	2–16	318	1	8	8.43(8)	11.26(8)	9.63(8)	11.76(8)
		CO <sub>2</sub> -KCl-H <sub>2</sub> O	2–16	318	1.5	8	2.93(8)	3.32(8)	13.78(8)	15.39(8)
2013	Tong et al. <sup>39</sup>	CO <sub>2</sub> -CaCl <sub>2</sub> -H <sub>2</sub> O	1.5–38	308–424	1–5	36	7.36(36)	6.73(24) <sup>b</sup>	4.85(24) <sup>b</sup>	4.69(24) <sup>c</sup>
		CO <sub>2</sub> -MgCl <sub>2</sub> -H <sub>2</sub> O	1.2–35	308–424	1–5	39	5.14(39)	6.14(26) <sup>b</sup>	5.67(26) <sup>b</sup>	5.83(26) <sup>c</sup>
2014	This study	CO <sub>2</sub> -CaCl <sub>2</sub> -H <sub>2</sub> O	15	323–423	0.33–2	18	0.88(18)	2.13(18)	3.61(18)	3.61(18)
		CO <sub>2</sub> -Na <sub>2</sub> SO <sub>4</sub> -H <sub>2</sub> O		323–423	0.33–2	18	0.75(18)	8.04(18)	7.50(3)	15.90(18)
		CO <sub>2</sub> -MgCl <sub>2</sub> -H <sub>2</sub> O		323–423	0.33–2	18	0.83(18)	2.30(18)	3.49(18)	3.20(18)
		CO <sub>2</sub> -KCl-H <sub>2</sub> O		323–423	0.5–4.5	18	0.33(18)	4.21(18)	14.91(18)	16.71(18)
Overall AAD % for each single-salt system (Including this study)		CO <sub>2</sub> -CaCl <sub>2</sub> -H <sub>2</sub> O					4.3(238)	5.9(224)	5.3(210)	5.5(220)
		CO <sub>2</sub> -Na <sub>2</sub> SO <sub>4</sub> -H <sub>2</sub> O					3.9(296)	13.2(287)	11.8(41)	27.1(277)
		CO <sub>2</sub> -MgCl <sub>2</sub> -H <sub>2</sub> O					3.8(87)	6.1(73)	5.5(69)	3.9(73)
		CO <sub>2</sub> -KCl-H <sub>2</sub> O					2.3(307)	4.9(307)	14.7(300)	12.4(305)
Overall AAD % Experimental data <i>P-T-x</i> coverage							3.6	7.5	9.3	12.2
							100%	96%	67%	94%

The numbers in parentheses stand for the number of experimental data evaluated by each model. “N/A” in the table denotes the *P-T-x* region of the experimental data beyond the capacity of the corresponding model.

<sup>a</sup>Indicates the experimental data taken from large the data compilation by Scharlin.<sup>40</sup>

<sup>b</sup>The experimental *P-T-x* points at *m*<sub>CaCl<sub>2</sub></sub> > 3 mol kg<sup>−1</sup> were removed from the comparison for both the OLI and SP2010 model due to relatively large AAD % for these models at high CaCl<sub>2</sub> concentration.

<sup>c</sup>The experimental *P-T-x* points at *m*<sub>CaCl<sub>2</sub></sub> > 4.5 mol kg<sup>−1</sup> were removed due to the DS2006 model is limited to 4.5 mol kg<sup>−1</sup> salt molality.

<sup>d</sup>Calculations made by OLI Studio 9.0.6 are under the following conditions: (1) enable the second liquid phase, (2) use MSE model, (3) stream inflows contains 55.51 mol water and 5 mol CO<sub>2</sub>.

be solved simultaneously using the Newton Raphson method with respect to *m*<sub>CO<sub>2</sub></sub>. The essential aspects of the phase equilibrium calculation are discussed in detail in Zhao et al.<sup>10</sup> In the following paragraphs, we present a general method to evaluate Pitzer model parameters, which enable the calculation of CO<sub>2</sub> solubility for different CO<sub>2</sub>-salt-H<sub>2</sub>O systems within the same thermodynamic framework.

The calculation of CO<sub>2</sub> solubility in aqueous salt solutions other than NaCl is achieved by fitting Pitzer model parameters to experimental CO<sub>2</sub> solubility for each CO<sub>2</sub>-salt-H<sub>2</sub>O system. Three parameters (*B*<sub>CO<sub>2</sub>-salt</sub>, *C*<sub>CO<sub>2</sub>-CO<sub>2</sub>-salt</sub>, and  $\xi_{\text{nca}}$ ) are needed to accurately correlate the experimental CO<sub>2</sub> solubility data for each CO<sub>2</sub>-salt-H<sub>2</sub>O system. Among these parameters, the combined Pitzer interaction parameters (*B*<sub>CO<sub>2</sub>-salt</sub> and *C*<sub>CO<sub>2</sub>-CO<sub>2</sub>-salt</sub>) can be written for any salt species as<sup>21</sup>

$$B_{\text{CO}_2-\text{salt}} = v^+ \lambda_{\text{nc}} + v^- \lambda_{\text{na}} \quad (5)$$

$$C_{\text{CO}_2-\text{CO}_2-\text{salt}} = v^+ \mu_{\text{nnc}} + v^- \mu_{\text{nna}} \quad (6)$$

where  $\lambda_{\text{nc}}$  and  $\lambda_{\text{na}}$  are the Pitzer neutral-cation and neutral-anion binary ion interaction parameters, respectively;  $\mu_{\text{nnc}}$  and  $\mu_{\text{nna}}$  are the Pitzer neutral-neutral-cation and neutral-neutral-anion triple ion interaction parameters, respectively. Subsequently, the Pitzer equation for activity coefficient of dissolved CO<sub>2</sub> [Appendix, Eq. A1] can be simplified as

$$\ln \gamma_{\text{CO}_2} = 2m_{\text{CO}_2} \lambda_{\text{nn}} + 3m_{\text{CO}_2}^2 \mu_{\text{nnn}} + 2B_{\text{CO}_2-\text{salt}} m_{\text{salt}} + v^+ v^- m_{\text{salt}}^2 \xi_{\text{nca}} + 6m_{\text{CO}_2} m_{\text{salt}} C_{\text{CO}_2-\text{CO}_2-\text{salt}} \quad (7)$$

where  $\lambda_{\text{nn}}$  and  $\mu_{\text{nnn}}$  are the Pitzer pure neutral component interaction parameters;<sup>10</sup> and  $\xi_{\text{nca}}$  is the Pitzer tripe-ion



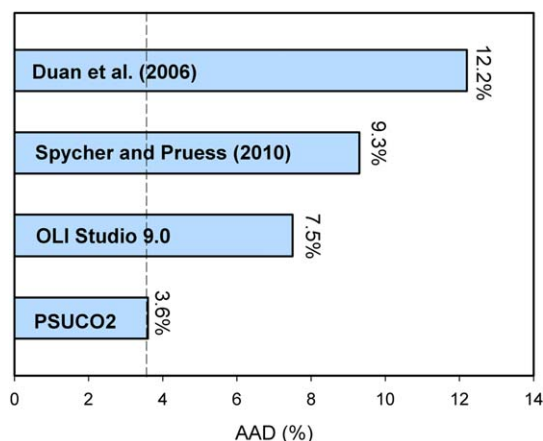


**Figure 1.** The AAD % of the calculated  $\text{CO}_2$  solubility values in aqueous  $\text{CaCl}_2$ ,  $\text{Na}_2\text{SO}_4$ ,  $\text{MgCl}_2$ , and  $\text{KCl}$  solutions by different models compared with the experimental data (all available experimental data listed in Table 4).

[Color figure can be viewed in the online issue, which is available at [wileyonlinelibrary.com](http://wileyonlinelibrary.com).]

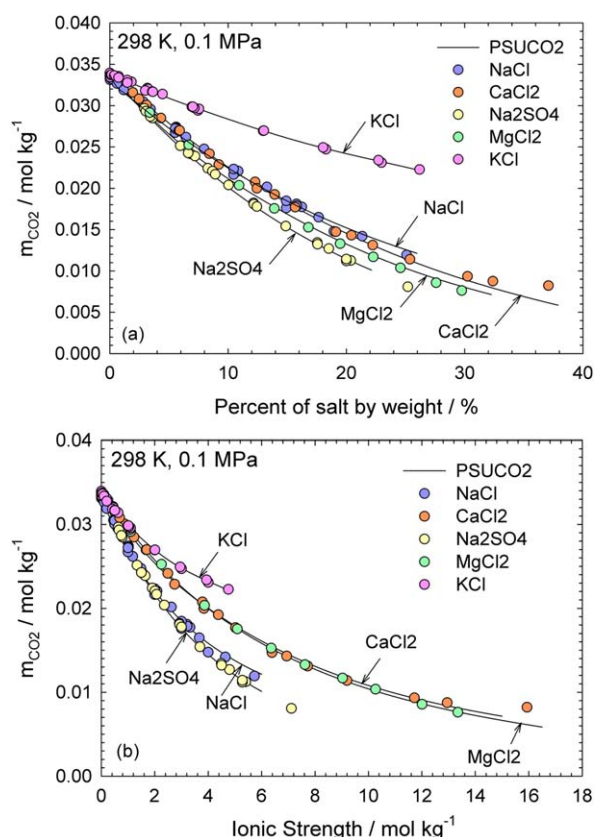


**Figure 2.** (a,b). Comparison of the experimental  $\text{CO}_2$  solubility<sup>23,26,31,35–38,40</sup> in various aqueous salt solutions at 298.15 K and 0.1 MPa based on different concentration scales: (a) percent of salt by weight; (b) ionic strength.

Solid lines represent the calculated values from the PSUCO2 model. [Color figure can be viewed in the online issue, which is available at [wileyonlinelibrary.com](http://wileyonlinelibrary.com).]

interaction parameter. For  $\text{CO}_2$ - $\text{H}_2\text{O}$  system, Eq. 7 can be reduced to Eq. 8 by setting the parameters  $B_{\text{CO}_2\text{-salt}}$ ,  $\xi_{\text{nca}}$ , and  $C_{\text{CO}_2\text{-CO}_2\text{-salt}}$  equal to zero

$$\ln \gamma_{\text{CO}_2}^0 = 2m_{\text{CO}_2}^0 \lambda_{\text{nn}} + 3(m_{\text{CO}_2}^0)^2 \mu_{\text{nnn}} \quad (8)$$

where  $\gamma_{\text{CO}_2}^0$  and  $m_{\text{CO}_2}^0$  are the activity coefficients of dissolved  $\text{CO}_2$  and solubility of  $\text{CO}_2$  ( $\text{CO}_2$  molality) in the  $\text{CO}_2$ - $\text{H}_2\text{O}$  system. The combined Pitzer interaction parameters  $B_{\text{CO}_2\text{-salt}}$  and  $C_{\text{CO}_2\text{-CO}_2\text{-salt}}$  in Eq. 7 were determined using experimental  $\text{CO}_2$  solubility in both pure water and aqueous single-salt solutions. To evaluate these two parameters, we made an assumption that the chemical potentials of  $\text{CO}_2$  in the  $\text{CO}_2$ - $\text{H}_2\text{O}$  and  $\text{CO}_2$ -salt- $\text{H}_2\text{O}$  systems are the same at a given  $P$ - $T$  condition based on the similar approach used by Akinfiev and Diamond.<sup>21</sup> At

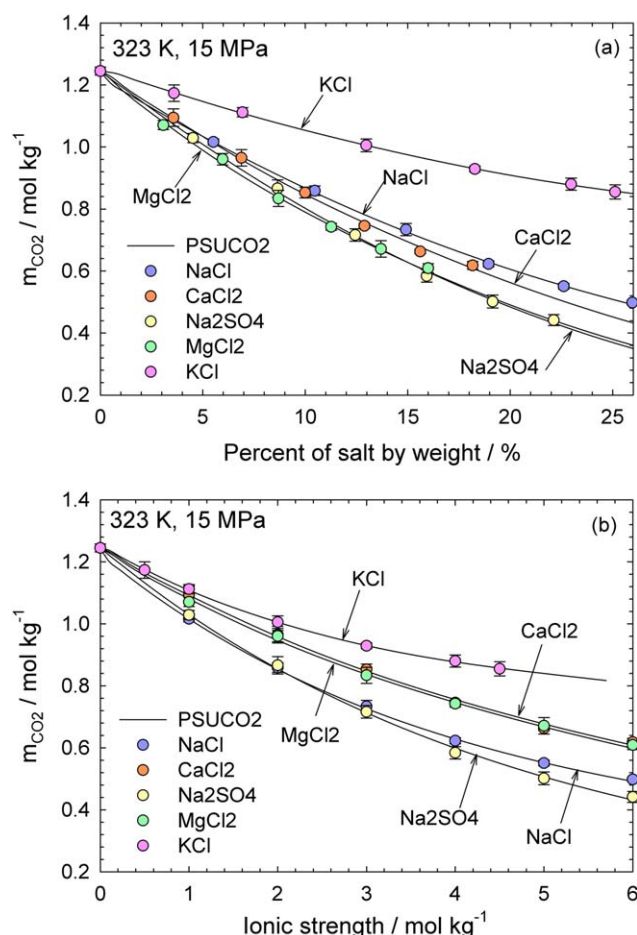


**Figure 3.** (a,b). Comparison of the experimental  $\text{CO}_2$  solubility (this study) in different aqueous salt solutions based on different concentration scales at 323 K and 15 MPa (the comparison at 373 and 423 K were not shown due to the similar pattern as that in 323 K, but the calculated solubility curves at those temperatures become more closer to each other than 323 K): (a) percent of salt by weight; (b) ionic strength.

Experimental  $\text{CO}_2$  solubility in aqueous  $\text{NaCl}$  solutions is taken from Zhao et al.<sup>10</sup> Solid lines represent the calculated values from the PSUCO2 model. [Color figure can be viewed in the online issue, which is available at [wileyonlinelibrary.com](http://wileyonlinelibrary.com).]

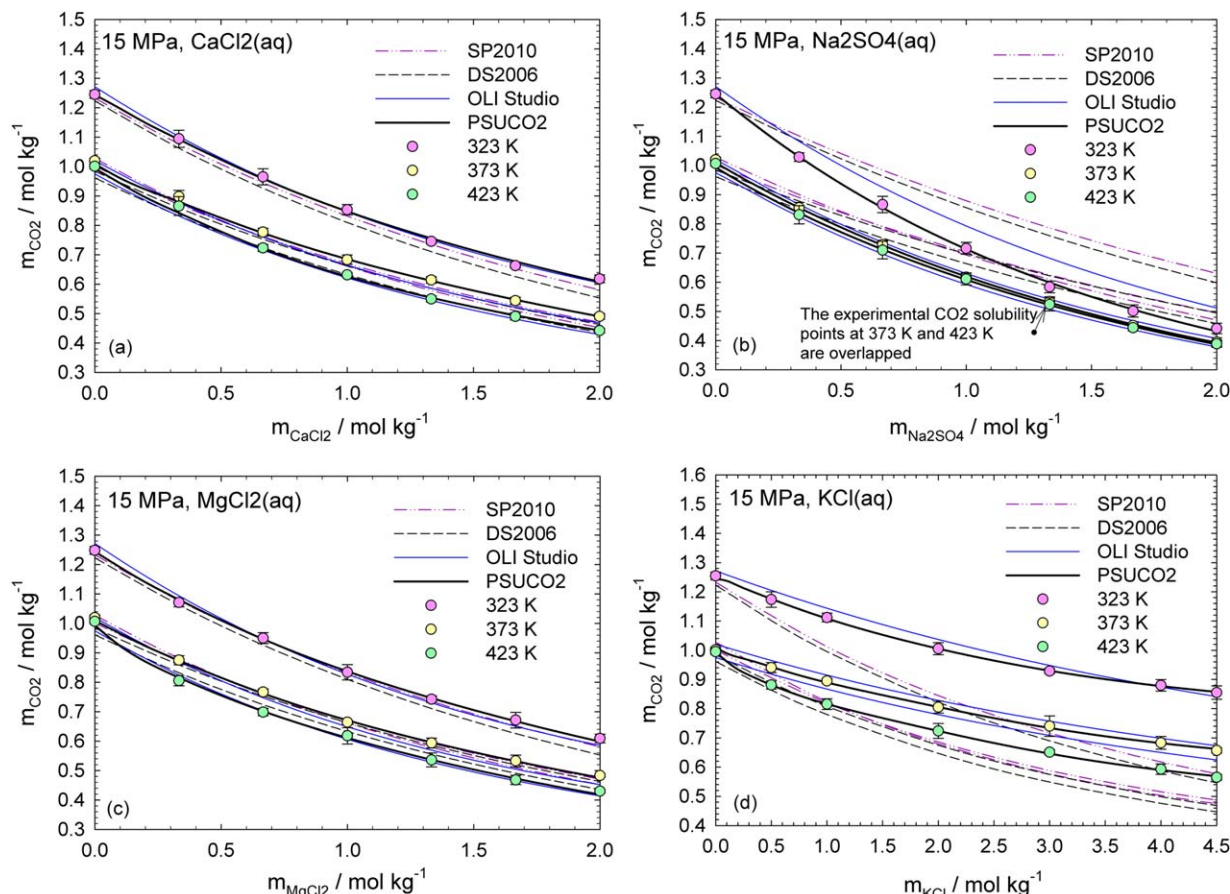


**Figure 4. (a–d). Comparison of model calculated values against the experimental CO<sub>2</sub> solubility (this study): (a) CO<sub>2</sub>–CaCl<sub>2</sub>–H<sub>2</sub>O system; (b) CO<sub>2</sub>–Na<sub>2</sub>SO<sub>4</sub>–H<sub>2</sub>O system; (c) CO<sub>2</sub>–MgCl<sub>2</sub>–H<sub>2</sub>O system (d) CO<sub>2</sub>–KCl–H<sub>2</sub>O system.**

[Color figure can be viewed in the online issue, which is available at [wileyonlinelibrary.com](http://wileyonlinelibrary.com).]

equilibrium, the chemical potential of CO<sub>2</sub> in the CO<sub>2</sub>-rich phase is equal to that in the aqueous phase, given by  $\mu_{\text{CO}_2}^{(g)} = \mu_{\text{CO}_2}^{(\text{aq})}$  for the CO<sub>2</sub>–H<sub>2</sub>O system and  $\mu_{\text{CO}_2}^{(g)} = \mu_{\text{CO}_2}^{(\text{aq})}$  for the CO<sub>2</sub>–salt–H<sub>2</sub>O system. In fact, the chemical potentials of CO<sub>2</sub> between the salt-bearing and salt-free systems are different. However, assuming that  $\mu_{\text{CO}_2}^{(g)} = \mu_{\text{CO}_2}^{(\text{aq})}$  results in a mean error of about 0.3% of calculated CO<sub>2</sub> solubility in the aqueous phase,<sup>21</sup> so this assumption is not significantly impactful to the overall model results. Thus, the equality of CO<sub>2</sub> activity, between the CO<sub>2</sub>–H<sub>2</sub>O and CO<sub>2</sub>–salt–H<sub>2</sub>O systems ( $\mu_{\text{CO}_2}^{(g)} = \mu_{\text{CO}_2}^{(\text{aq})}$ ) can be represented as follows

$$\ln(m_{\text{CO}_2} \gamma_{\text{CO}_2}) = \ln(m_{\text{CO}_2}^{\circ} \gamma_{\text{CO}_2}^{\circ}) \quad (9)$$

Combining Eqs. 7, 8, and 9, the combined Pitzer interaction parameters  $B_{\text{CO}_2\text{--salt}}$  and  $C_{\text{CO}_2\text{--CO}_2\text{--salt}}$  (in Eq. 7) can be determined by fitting of Eq. 9 to the corresponding experimental CO<sub>2</sub> solubility data in both CO<sub>2</sub>–H<sub>2</sub>O and CO<sub>2</sub>–salt–H<sub>2</sub>O systems. As a results, the parameters  $B_{\text{CO}_2\text{--salt}}$  and  $C_{\text{CO}_2\text{--CO}_2\text{--salt}}$  for each CO<sub>2</sub>–salt–H<sub>2</sub>O system can be calculated in terms of the temperature, ionic strength, and coefficients  $a_1$  to  $a_5$

$$B_{\text{CO}_2\text{--salt}} = a_1 + a_2 \frac{100}{T - \theta} + a_3 \frac{T}{1000} + a_4 g(x) \quad (10)$$

$$C_{\text{CO}_2\text{--CO}_2\text{--salt}} = a_5 \quad (11)$$

where  $\theta = 228 \text{ K}$ ,  $g(x) = \frac{2}{x^2} (1 - (1+x)e^{-x})$ ,  $x = \alpha_1 I^{0.5}$ , and  $\alpha_1 = 2.0 \text{ kg}^{0.5} \text{ mol}^{-0.5}$ . The detailed data fitting procedure to estimate coefficients  $a_1$  to  $a_5$  is provided in Supporting

Information. The data fitting results of coefficients  $a_1$  to  $a_5$  are shown in Table 2.

In addition, through the comparison between model calculated results and the experimental data reported herein, we found that the parameter  $\xi_{\text{nca}}$  has a strong dependence on temperature and salt concentration, especially at high temperatures and low salt concentrations, but it is insensitive to the system pressure. Therefore, the Pitzer triple-ion interaction parameter  $\xi_{\text{nca}}$  (in Eq. 7) was calculated by performing a binary search for  $m_{\text{CO}_2}$  in the PSUCO2 model until consistency between the calculated and experimental values was obtained. The results of  $\xi_{\text{nca}}$  determined in this manner are listed in Table 3. By assuming independence of pressure,  $\xi_{\text{nca}}$  at any  $P$ – $T$ – $x$  conditions can be obtained through an interpolation or extrapolation of the values listed in Table 3 for the corresponding CO<sub>2</sub>–salt–H<sub>2</sub>O system. The procedure is: (1) a cubic spline interpolation with a step of  $0.001 \text{ mol kg}^{-1}$  salt molality was used to get the relationship between  $\xi_{\text{nca}}$  and salt concentration (molality) at a constant temperature; and then (2) the linear interpolation was applied to calculate  $\xi_{\text{nca}}$  at any targeted  $P$ – $T$ – $x$  point. Finally, using the calculated results of  $\beta_{\text{ca}}^{(0)}$ ,  $\beta_{\text{ca}}^{(1)}$ , and  $C_{\text{ca}}^{\phi}$  (Supporting Information) along with the parameters  $B_{\text{CO}_2\text{--salt}}$ ,  $C_{\text{CO}_2\text{--CO}_2\text{--salt}}$ , and  $\xi_{\text{nca}}$ , the previously developed CO<sub>2</sub> solubility model for the aqueous NaCl solution was effectively extended to the aqueous CaCl<sub>2</sub>, Na<sub>2</sub>SO<sub>4</sub>, MgCl<sub>2</sub>, KCl solutions.

In Table 4, the modeling results of CO<sub>2</sub> solubility in the aqueous phase from various models (PSUCO2, SP2010, DS2006, and OLI) were compared to the experimental

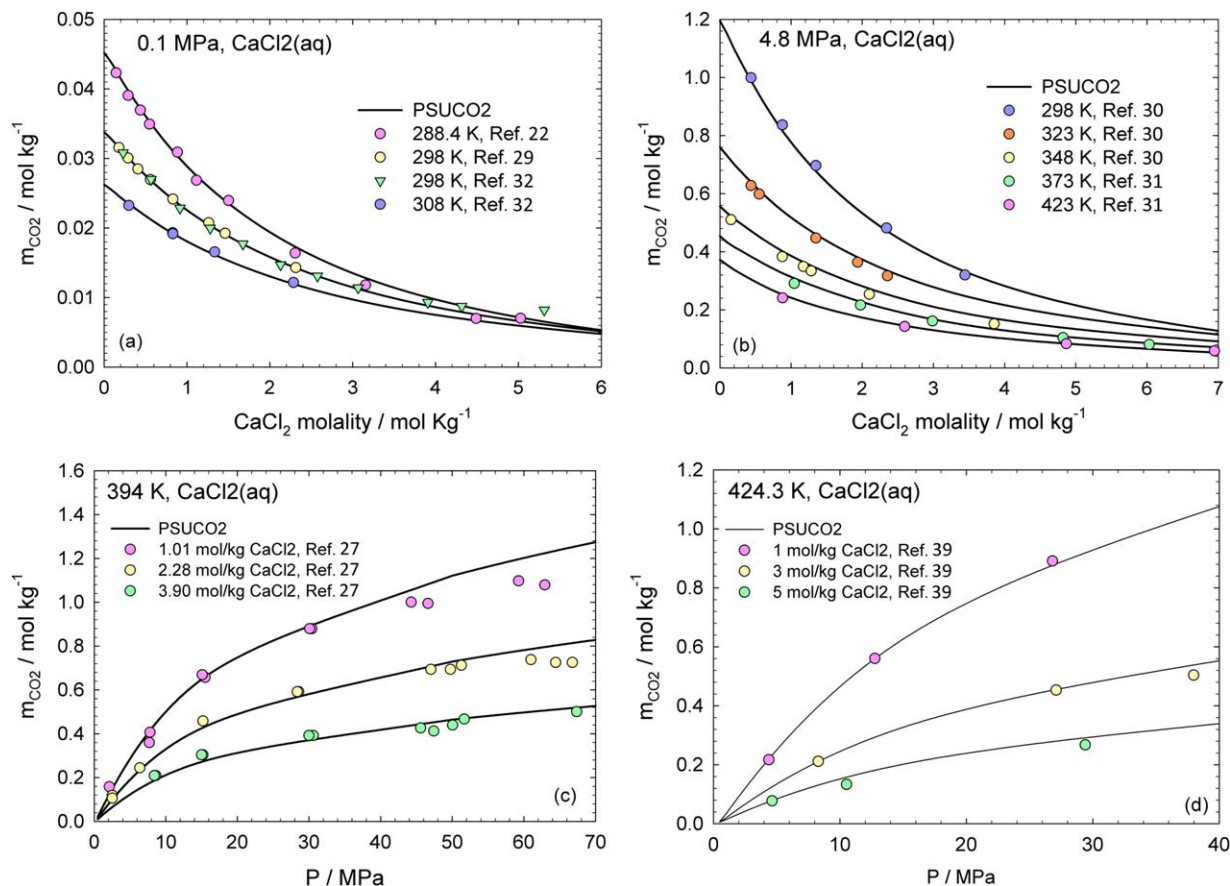


**Figure 5. (a–d). Comparison of model calculations against the experimental  $\text{CO}_2$  solubility<sup>22–26,35,39</sup> in aqueous  $\text{CaCl}_2$  solutions.**

(a) 0.1 MPa, 288–308 K, and 0.14–5.31 mol  $\text{kg}^{-1}$   $\text{CaCl}_2$ ; (b) 4.8 MPa, 298–423 K, and 0.16–6.95 mol  $\text{kg}^{-1}$   $\text{CaCl}_2$ ; (c) 2.1–71.2 MPa, 394 K, and 1.01–3.90 mol  $\text{kg}^{-1}$   $\text{CaCl}_2$ ; (d) 4.4–38 MPa, 424.4 K, and 1–5 mol  $\text{kg}^{-1}$   $\text{CaCl}_2$ . [Color figure can be viewed in the online issue, which is available at [wileyonlinelibrary.com](http://wileyonlinelibrary.com).]

data<sup>14,22–40</sup> in terms of average absolute deviation (AAD %), which is defined as below

$$\text{AAD}(\%) = \frac{100}{N_p} \sum_{i=1}^N \left| \frac{m_{\text{CO}_2,i}^{\text{calc}} - m_{\text{CO}_2,i}^{\text{exp}}}{m_{\text{CO}_2,i}^{\text{exp}}} \right| \% \quad (12)$$

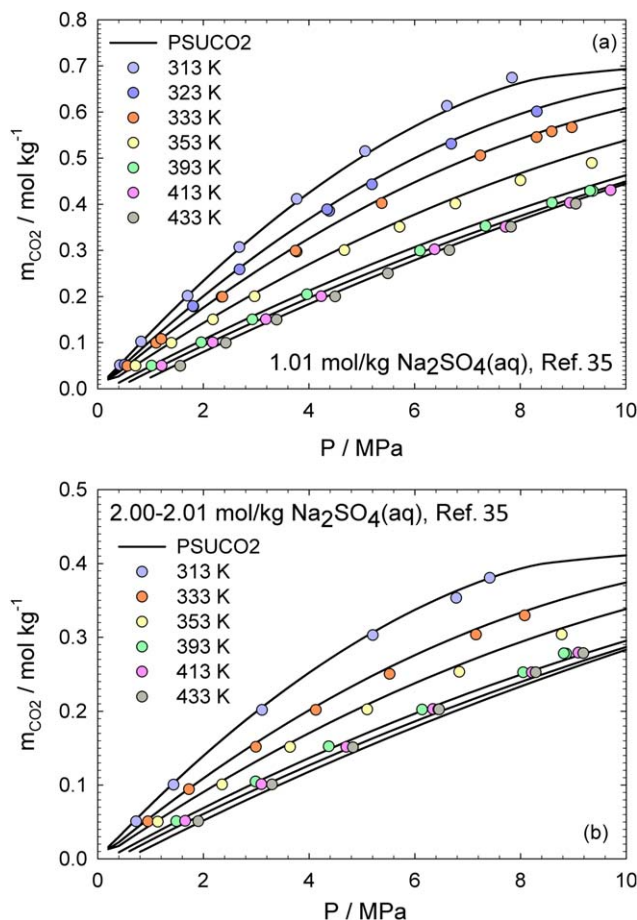
where  $m_{\text{CO}_2,i}^{\text{calc}}$  represents the calculated  $\text{CO}_2$  solubility values from the  $\text{CO}_2$  solubility models (PSUCO2, SP2010, DS2006, and OLI);  $m_{\text{CO}_2,i}^{\text{exp}}$  denotes the experimental  $\text{CO}_2$  solubility taken from literature and obtained in this study; and  $N$  means the total number of experimental data in each work. Table 4 demonstrates that the PSUCO2 model predicts the  $\text{CO}_2$  solubility in aqueous  $\text{CaCl}_2$ ,  $\text{Na}_2\text{SO}_4$ ,  $\text{MgCl}_2$ , and  $\text{KCl}$  solutions with a high degree of accuracy over a wide  $P$ - $T$ - $x$  range [288–433 K, 1–71 MPa, and ionic strength up to 20.7 mol  $\text{kg}^{-1}$  for  $\text{CaCl}_2(\text{aq})$ , 7.2 mol  $\text{kg}^{-1}$  for  $\text{Na}_2\text{SO}_4(\text{aq})$ , 15 mol  $\text{kg}^{-1}$  for  $\text{MgCl}_2(\text{aq})$ , and 4.8 mol  $\text{kg}^{-1}$  for  $\text{KCl}(\text{aq})$ ]. Although there is a lack of experimental  $\text{CO}_2$  solubility to validate the model performance at the pressures higher than 71 MPa and temperatures above 433 K, the proposed PSUCO2 model can still be safely extended to 150 MPa and 523 K due to the following reasons: (1) the model is based on a sound thermodynamic framework, which is validated by reliable experimental up to 200 MPa and 573 K for the  $\text{CO}_2$ - $\text{H}_2\text{O}$  binary system;<sup>10</sup> and (2) the same thermodynamic framework is also validated by reliable experimental  $\text{CO}_2$  solubility in the aqueous phase for the  $\text{CO}_2$ - $\text{NaCl}$ - $\text{H}_2\text{O}$  system up to 150 MPa and 573 K.<sup>10</sup> In addition to Table 4,

Figure 1 clearly indicates that the proposed PSUCO2 model provides the best performance in calculating the  $\text{CO}_2$  solubility in all  $\text{CO}_2$ -salt- $\text{H}_2\text{O}$  systems investigated in this study relative to the published models (SP2010, DS2006, and OLI). The updated model is named as PSUCO2 and is available as an Internet-based computational tool (Supporting Information).

## Discussion

At atmospheric pressure, Li and Tsui<sup>41</sup> measured  $\text{CO}_2$  solubility in aqueous  $\text{NaCl}$  solution (0.6413 mol  $\text{kg}^{-1}$   $\text{NaCl}$ ) and acidified seawater (with 10, 20, and 29‰ Chlorinity) at the temperature range from 273.85 to 303.15 K. Based on the obtained experimental results, Li and Tsui<sup>41</sup> concluded that the Buch's assumption<sup>42</sup>—the effect of a given weight of sea salts on solubility of  $\text{CO}_2$  is the same as that of an identical weight of  $\text{NaCl}$ —is proved to be valid. A question arises when extending Li and Tsui's conclusion from sea salt to any salt species—is the effect of a given weight of any salt (or mixed-salt) on solubility of  $\text{CO}_2$  still the same as that of an identical weight of  $\text{NaCl}$ ? The answer is no. In this study, we have experimentally demonstrated that  $\text{CO}_2$  solubility in aqueous solutions with different salt species are significantly different at 15 MPa, whether the solutions have the same percent of salt by weight or have the same ionic strength. This observation is also substantiated by experimental  $\text{CO}_2$  solubility data<sup>23,24</sup> at ambient conditions (Figure 2). Figures





**Figure 6. (a,b).** Comparison of the model calculations against the experimental  $\text{CO}_2$  solubility<sup>29</sup> in aqueous  $\text{Na}_2\text{SO}_4$  solutions.

(a) 0.4–9.7 MPa, 313–433 K, and  $1 \text{ mol kg}^{-1} \text{ Na}_2\text{SO}_4$ ; (b) 0.7–9.2 MPa, 313–433 K, and  $2 \text{ mol kg}^{-1} \text{ Na}_2\text{SO}_4$ . [Color figure can be viewed in the online issue, which is available at [wileyonlinelibrary.com](http://wileyonlinelibrary.com).]

2b and 3b show that the magnitude of  $\text{CO}_2$  solubility in aqueous salt solutions follows a decreasing sequence of  $m_{\text{CO}_2}^{\text{KCl}} > m_{\text{CO}_2}^{\text{CaCl}_2} > m_{\text{CO}_2}^{\text{MgCl}_2} > m_{\text{CO}_2}^{\text{NaCl}} > m_{\text{CO}_2}^{\text{Na}_2\text{SO}_4}$  based on the same ionic strength.

The ion-water molecule interactions dominate the  $\text{CO}_2$  solubility behavior in different aqueous salt solutions. For example, on the basis of the number of ions produced when strong electrolyte dissociates in solution,  $\text{MgCl}_2$  and  $\text{CaCl}_2$  are the same type electrolytes (1-2 type). The measured solubility of  $\text{CO}_2$  in  $\text{CaCl}_2(\text{aq})$  and in  $\text{MgCl}_2(\text{aq})$  are quite close in a wide  $P$ - $T$ - $x$  range (Figures 2 and 3), but the measured  $\text{CO}_2$  solubility in  $\text{CaCl}_2(\text{aq})$  is always slightly greater than that in  $\text{MgCl}_2(\text{aq})$ . Whereas, the solubility of  $\text{CO}_2$  in aqueous  $\text{NaCl}$  solution is considerably smaller than that in aqueous  $\text{KCl}$  solution given that these two salts share the same electrolyte type (1-1 type; Figures 2 and 3). The studies of the ion hydration and ion-water molecule interactions<sup>43,44</sup> demonstrated that small ions of high charge density bind water molecules strongly, whereas large ions of low charge density bind water molecules weakly. Thus, the high charge density ions have strong influence on water structure, which determines the capacity of the aqueous phase to trap dissolved  $\text{CO}_2$ . Based on the experimental results, if two single-salt aqueous solutions have the same

type of electrolyte (e.g., 2-1 or 1-1 type) and share the same anion (e.g.,  $\text{Cl}^-$ ), a cation with greater charge density (a smaller radii and a greater charge number) has more significant salting-out effect on dissolved  $\text{CO}_2$  than that with smaller charge density. For example, the charge density of  $\text{Mg}^{2+}$  is slightly greater than that of  $\text{Ca}^{2+}$  (same charge number but  $\text{Mg}^{2+}$  has a smaller radius than  $\text{Ca}^{2+}$ ),<sup>45</sup> as a result, the amount of  $\text{CO}_2$  dissolved in aqueous  $\text{MgCl}_2$  is less than that in aqueous  $\text{CaCl}_2$  solution at the same ionic strength. The similar situation occurs for the  $\text{CO}_2$  solubility in aqueous  $\text{NaCl}$  and  $\text{KCl}$  solutions.  $\text{Na}^+$  has a significantly greater charge density than  $\text{K}^+$ , thus the  $\text{CO}_2$  solubility in aqueous  $\text{NaCl}$  solution is considerably less than that in aqueous  $\text{KCl}$  solutions.

Figure 4 and Table 4 (row 19) show that SP2010 and DS2006 models predict the experimental data obtained herein quite well for the  $\text{CO}_2$ - $\text{CaCl}_2$ - $\text{H}_2\text{O}$  (Figure 4a) and  $\text{CO}_2$ - $\text{MgCl}_2$ - $\text{H}_2\text{O}$  (Figure 4c) systems, however, these models (SP2010 and DS2006) predict the measured  $\text{CO}_2$  solubility in aqueous  $\text{Na}_2\text{SO}_4$  and  $\text{KCl}$  solutions with a large error (Figures 4b, d). The SP2010 and DS2010 models use the same type of simplified Pitzer equation to calculate aqueous phase activity coefficients.<sup>7</sup> Because the similar activity equation is used in both DS2006 and SP2010 models, the

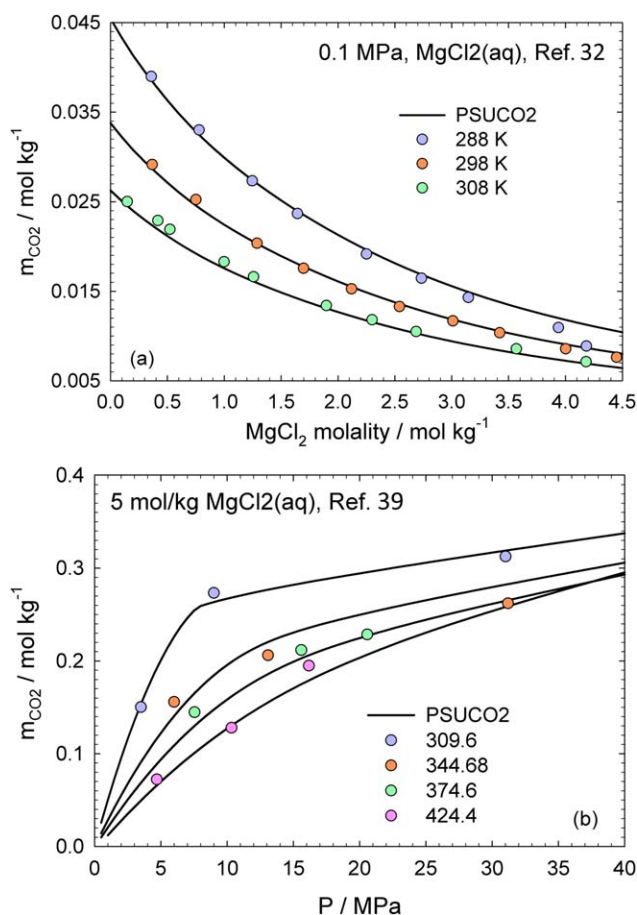


**Figure 7. (a,b).** Comparison of the model calculations against the experimental  $\text{CO}_2$  solubility<sup>26,39</sup> in aqueous  $\text{MgCl}_2$  solutions.

(a) 0.1 MPa, 288–303 K, and  $0.15$ – $4.45 \text{ mol kg}^{-1} \text{ MgCl}_2$ ; (b)  $3.5$ – $31.2 \text{ MPa}$ ,  $309.6$ – $424.4 \text{ mol kg}^{-1} \text{ MgCl}_2$ . [Color figure can be viewed in the online issue, which is available at [wileyonlinelibrary.com](http://wileyonlinelibrary.com).]



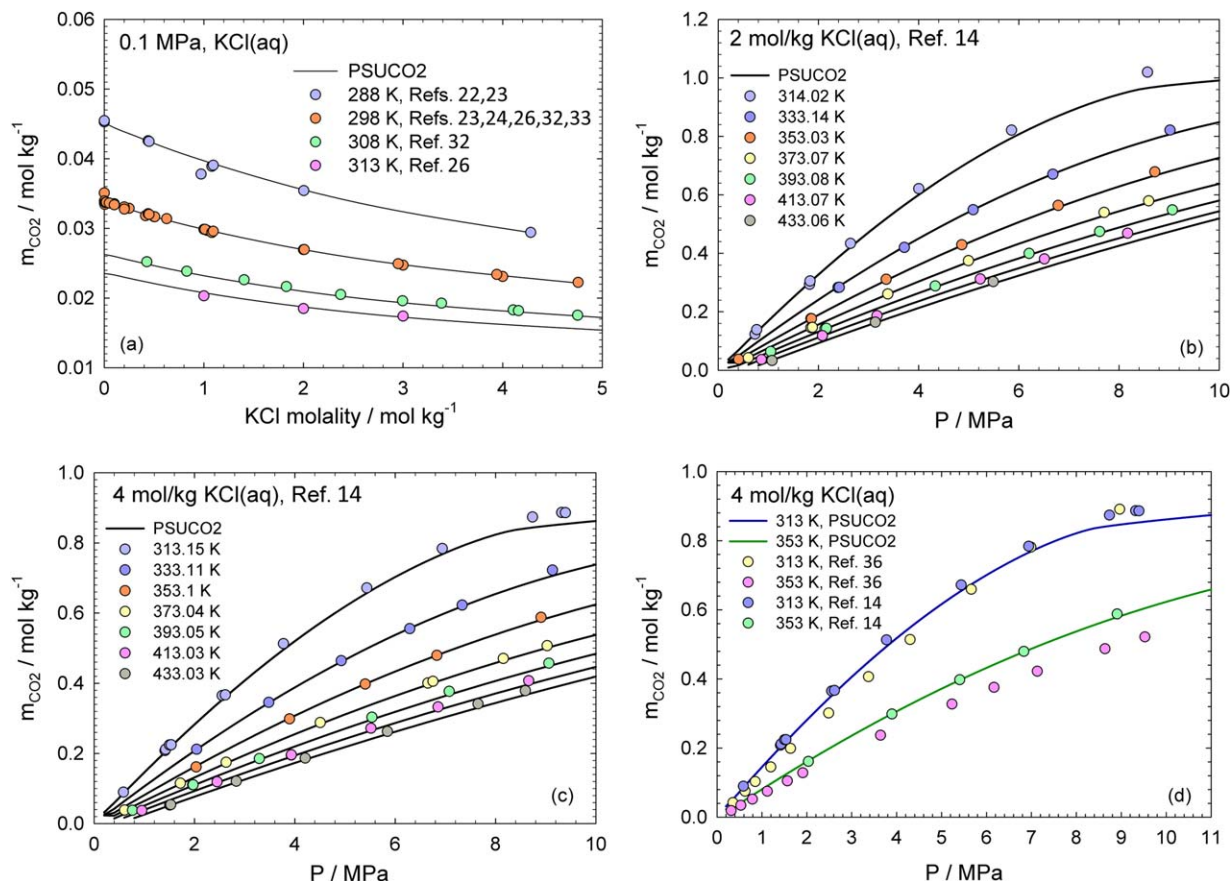


**Figure 8. (a–d). Comparison of the model calculations against the experimental  $\text{CO}_2$  solubility<sup>14,26,31,35–37,33,34</sup> in aqueous KCl solutions.**

(a) 0.1 MPa, 288–313 K, 0–4.75 mol kg<sup>-1</sup> KCl; (b) 0.4–9.1 MPa, 314–433 K, and 2 mol kg<sup>-1</sup> KCl; (c) 0.6–9.4 MPa, 313–433 K, and 4 mol kg<sup>-1</sup> KCl; (d) Comparison of the experimental  $\text{CO}_2$  solubility between Pérez-Salado Kamps<sup>14</sup> and Kiepe et al.<sup>34</sup> at the same  $P$ - $T$ - $x$  conditions, the modeling results are in excellent agreement with the experimental results reported by Pérez-Salado Kamps.<sup>14</sup> [Color figure can be viewed in the online issue, which is available at [wileyonlinelibrary.com](http://wileyonlinelibrary.com).]

calculated  $\text{CO}_2$  solubilities in aqueous NaCl and KCl solutions, as well as in aqueous  $\text{CaCl}_2$  and  $\text{MgCl}_2$  solutions, are identical from these models. OLI Studio 9.0.6 performs very well in calculating  $\text{CO}_2$  solubility in the aqueous KCl,  $\text{CaCl}_2$ , and  $\text{MgCl}_2$  solutions when compared with our experimental results, but OLI calculated results for the  $\text{CO}_2$ - $\text{Na}_2\text{SO}_4$ - $\text{H}_2\text{O}$  system also deviate from the experimental  $\text{CO}_2$  solubility measured in this study (Figure 4b).

The calculated  $\text{CO}_2$  solubility from the PSUCO2 model shows a remarkable agreement when compared with the previously published experimental data in various  $\text{CO}_2$ -salt- $\text{H}_2\text{O}$  system (Figures 5–8). However, at same  $P$ - $T$ - $x$  conditions, a large discrepancy of experimental results for the  $\text{CO}_2$ -KCl- $\text{H}_2\text{O}$  system between Pérez-Salado Kamps et al.<sup>14</sup> and Kiepe et al.<sup>34</sup> was observed, and the calculated results from the PSUCO2 model support the experimental  $\text{CO}_2$  solubility reported by Pérez-Salado Kamps et al. (Figure 8d).<sup>14</sup>

The  $\text{H}_2\text{O}$  solubility in the  $\text{CO}_2$ -rich phase can also be calculated by the proposed PSUCO2 model. Reliable experimental data are desirable to evaluate the model performance at elevated temperatures and pressures. At high temperatures and pressures, the experimental  $\text{H}_2\text{O}$  solubility in the  $\text{CO}_2$ -rich phase reported by Takenouchi and Kennedy<sup>46</sup> and Tödheide and Franck<sup>47</sup> are significantly different. Later on, to resolve this discrepancy, Mather and Franck<sup>48</sup> used the so-called “synthetic” experimental method to study the phase equilibria of the  $\text{CO}_2$ - $\text{H}_2\text{O}$  system. Initially, known amounts

of  $\text{CO}_2$  and  $\text{H}_2\text{O}$  are loaded into an autoclave (with a sapphire window). By heating the components in the autoclave at constant volume, homogeneous single-phase conditions can be observed through the window. By this means, Mather and Franck stated their measured dew points (at 498.15–546.15 K and 1100–2640 bar) of  $\text{H}_2\text{O}$  in the  $\text{CO}_2$ -rich phase support the experimental results of Tödheide and Franck.<sup>47</sup> In Figure 9a, the calculated  $\text{H}_2\text{O}$  solubility in the  $\text{CO}_2$ -rich phase among the different models (PSUCO2, OLI, and SP2010) were compared with the experimental data<sup>46,47,49,50</sup> at 298 and 423 K and up to 50 MPa. At 298 K, the differences among the three models are rather small (Figure 9a). All three models are capable of predicting the phase change (Figure 9a, enlarged view) from gaseous to liquid  $\text{CO}_2$ -rich phase<sup>15</sup> at 298 K as compared with the experimental data.<sup>49,50</sup> At 423 K, the PSUCO2 and SP2010 models agree well with the experimental data,<sup>47</sup> but the calculated results from OLI gradually deviate from the results of the other models (PSUCO2 and SP2010) in predicting  $\text{H}_2\text{O}$  solubility in the  $\text{CO}_2$ -rich phase at 423 K when pressure increases from 15 to 50 MPa (Figure 9a).

For a  $\text{CO}_2$ -salt- $\text{H}_2\text{O}$  system, the PSUCO2 model calculated results (as shown in Figure 9b) demonstrate that the different salt species in the aqueous phase will influence the  $\text{H}_2\text{O}$  solubility in the  $\text{CO}_2$ -rich phase. Based on comparison between Figures 9b and 9c, a larger activity of  $\text{H}_2\text{O}$  yields a greater solubility of  $\text{H}_2\text{O}$  in the  $\text{CO}_2$ -rich phase among

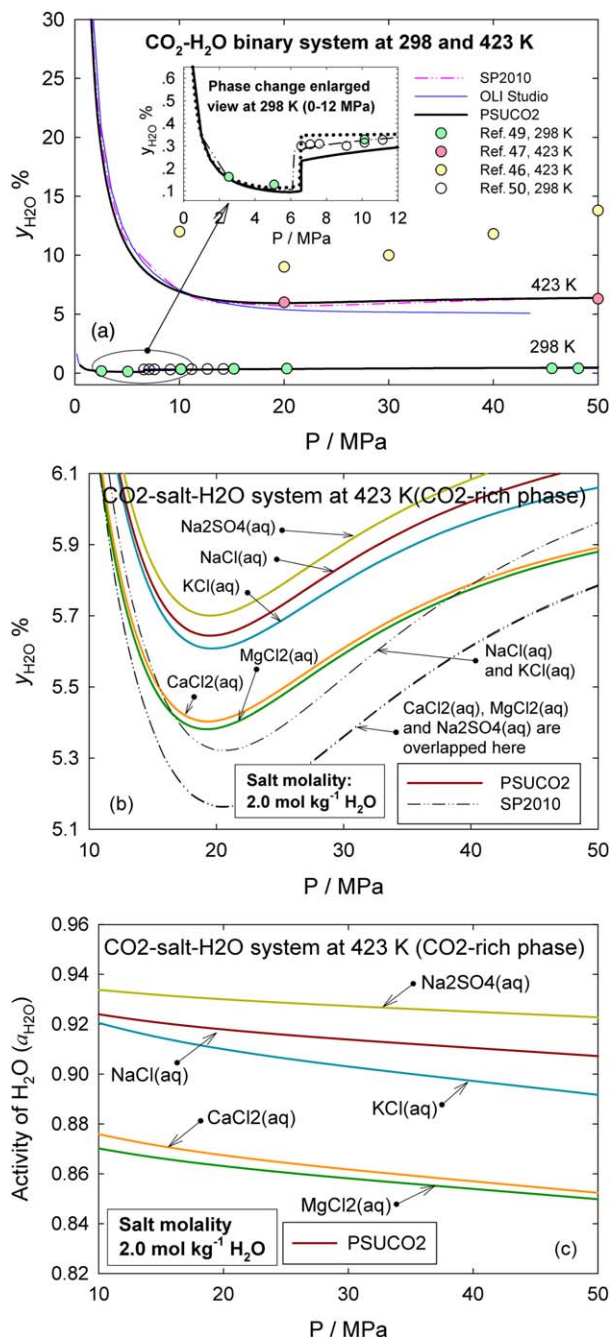


**Figure 9. (a–c). Comparison of the model calculated H<sub>2</sub>O solubility in the CO<sub>2</sub>-rich phase for different CO<sub>2</sub>-salt-H<sub>2</sub>O systems.**

(a) Comparison calculated H<sub>2</sub>O solubility in the CO<sub>2</sub>-rich phase for the binary CO<sub>2</sub>-H<sub>2</sub>O system by different models (SP2010, OLI, and PSUCO2); (b) Model calculated H<sub>2</sub>O solubility in the CO<sub>2</sub>-rich phase at 423 K in the CO<sub>2</sub>-salt-H<sub>2</sub>O systems. Given the same salt molality (e.g., 2 mol kg<sup>-1</sup>), the differences of H<sub>2</sub>O solubility in various single-salt aqueous solutions are quite large, whereas the SP2010 model reflects a relatively smaller variation of H<sub>2</sub>O contents in the CO<sub>2</sub>-rich phase caused by different salt species in the aqueous phase than does PSUCO2; (c) the PSUCO2 model calculated activity of H<sub>2</sub>O in the aqueous phase for different CO<sub>2</sub>-salt-H<sub>2</sub>O systems at 423 K. Calculations made by OLI Studio 9.0.6 in Fig. 9a are under following conditions: (1) enable the second liquid phase, (2) use MSE model, (3) stream inflows contains 55.5082 mol water and 5 mol CO<sub>2</sub>. [Color figure can be viewed in the online issue, which is available at [wileyonlinelibrary.com](http://wileyonlinelibrary.com).]

different CO<sub>2</sub>-salt-H<sub>2</sub>O systems. However, for the same salt species the increase of the H<sub>2</sub>O activity does not guarantee increased H<sub>2</sub>O solubility in the CO<sub>2</sub>-rich phase.

As described above, the Pitzer model is used to calculate the activity of dissolved CO<sub>2</sub> ( $a_{\text{CO}_2}$ ) and the activity of H<sub>2</sub>O ( $a_{\text{H}_2\text{O}}$ ) in a CO<sub>2</sub>-salt-H<sub>2</sub>O system. Once  $a_{\text{CO}_2}$  and  $a_{\text{H}_2\text{O}}$  in mixed electrolyte solutions are evaluated, the CO<sub>2</sub> solubility in mixed-salt aqueous solutions may be calculated within the same thermodynamic framework. However, while the Pitzer model provides the thermodynamic framework to calculate the activity coefficient of CO<sub>2</sub> (neutral species) in mixed electrolyte solutions, a detailed discussion of Pitzer equations agrees that when a salt mixture presents in the aqueous phase, the number of required parameters increases significantly in Pitzer equations.<sup>51</sup> These parameters must be determined by thermodynamic experimental data for multicomponent systems. However, for CO<sub>2</sub>-mixed-salt-H<sub>2</sub>O system, there is a lack of experimental data of CO<sub>2</sub> solubility in mixed-salt aqueous solutions (e.g., NaCl + CaCl<sub>2</sub>, NaCl + MgCl<sub>2</sub>, NaCl + KCl, CaCl<sub>2</sub> + MgCl<sub>2</sub>, CaCl<sub>2</sub> + Na<sub>2</sub>SO<sub>4</sub>, etc.), therefore, the approach using the Pitzer model to predict CO<sub>2</sub> solubility in mixed-salt aqueous solution at elevated temperatures and pressures is still not available for us.

However, based on the calculated CO<sub>2</sub> solubility in aqueous single-salt solutions, the CO<sub>2</sub> solubility in aqueous mixed-salt solution can be evaluated by the additivity rule of Setschenow coefficients for each single-salt species. The salting-out effect of single-salt species on dissolved CO<sub>2</sub> can be represented the Setschenow coefficient ( $K_s^i$ ), which is calculated by the classical Setschenow equation as below<sup>52</sup>

$$K_s^i = \frac{1}{C_s^i} \log \frac{C_{\text{CO}_2}^0}{C_{\text{CO}_2}^i} \quad (13)$$

where  $C_s^i$  is the molarity of the  $i$ th salt species in a single-salt electrolyte solution, mol L<sup>-1</sup>;  $C_{\text{CO}_2}^0$  is the CO<sub>2</sub> molarity in pure water, mol L<sup>-1</sup>; and  $C_{\text{CO}_2}^i$  is the CO<sub>2</sub> molarity in the single-salt aqueous solution with  $i$ th salt species. The proposed PSUCO2 model is capable of calculating Setschenow coefficients ( $K_s^{\text{NaCl}}$ ,  $K_s^{\text{MgCl}_2}$ ,  $K_s^{\text{CaCl}_2}$ ,  $K_s^{\text{Na}_2\text{SO}_4}$ , and  $K_s^{\text{KCl}}$ ) for corresponding single-salt aqueous solutions. The Setschenow coefficient of a mixed-salt solution ( $K_s^{\text{Mix}}$ ) can be evaluated using the additivity rule of Setschenow coefficients in each involved single-salt solution. The detailed method to calculate  $K_s^{\text{Mix}}$  based on the obtained  $K_s^{\text{NaCl}}$ ,  $K_s^{\text{MgCl}_2}$ ,  $K_s^{\text{CaCl}_2}$ ,  $K_s^{\text{Na}_2\text{SO}_4}$ , and  $K_s^{\text{KCl}}$  can be found in Zhao et al.<sup>53</sup>

## Conclusions

A new set of CO<sub>2</sub> solubility data in aqueous CaCl<sub>2</sub>, MgCl<sub>2</sub>, Na<sub>2</sub>SO<sub>4</sub>, and KCl solutions were measured at temperatures from 323 to 423 K, the ionic strengths from 0 to 6 mol kg<sup>-1</sup> and a pressure of 15 MPa. The comparisons of experimental results based on the same concentration scale (ionic strength or salt percent by weight) showed that (1) the solubility of CO<sub>2</sub> in aqueous solutions in the presence of different salt species are quite different; (2) the solubility of CO<sub>2</sub> in CaCl<sub>2</sub>(aq) and MgCl<sub>2</sub>(aq) solutions are close to each other; and (3) given the same type of electrolyte (with the same anion), a cation with greater charge density in the aqueous phase has more significant salting-out effect on dissolved CO<sub>2</sub> than that with smaller charge density.

The previously developed CO<sub>2</sub> solubility model for the CO<sub>2</sub>-NaCl-H<sub>2</sub>O system was extended to the systems of CO<sub>2</sub>-CaCl<sub>2</sub>-H<sub>2</sub>O, CO<sub>2</sub>-Na<sub>2</sub>SO<sub>4</sub>-H<sub>2</sub>O, CO<sub>2</sub>-MgCl<sub>2</sub>-H<sub>2</sub>O, and CO<sub>2</sub>-

KCl-H<sub>2</sub>O by fitting a new set of Pitzer model parameters for each system. Pitzer model provides highly-accurate correlation results of CO<sub>2</sub> solubility in single-salt aqueous solutions, however, the use of Pitzer model for mixed-salt aqueous system at elevated temperatures and pressures is not recommended due to too many model parameters need to be evaluated.

Comparisons against literature data reveal a clear improvement of the proposed PSUCO<sub>2</sub> model among the published models in predicting CO<sub>2</sub> solubility in aqueous single-salt solutions at temperatures from 288 to 433 K and pressures up to 71 MPa. The applicable *P-T-x* range of the proposed PSUCO<sub>2</sub> model is 288–523 K, 0.1–150 MPa, and salt concentration up to saturation conditions.

## Acknowledgments

This work was partly supported by the U.S. Department of Energy, the National Energy Technology Laboratory, and the Regional University Alliance (NETL-RUA) and the Energy Institute of College of Earth and Mineral Sciences at the Pennsylvania State University. We particularly thank Dr. Nikolay N. Akinfiev and Dr. Nicolas Spycher for the access to their computer codes. The authors thank Shimei Ma for her help in preparing the model comparison results.

## Notations

### Uppercase

AAD % = average absolute deviation

$A^\phi$  = Debye–Hückel slope for osmotic coefficient

$B_{\text{CO}_2\text{-salt}}$  = combined Pitzer interaction parameter for the CO<sub>2</sub>-salt-H<sub>2</sub>O system

$C_{\text{CO}_2\text{-CO}_2\text{-salt}}$  = combined Pitzer triple interaction parameter for the CO<sub>2</sub>-salt-H<sub>2</sub>O system

$C_{\text{ca}}C_{\text{ca}}^\phi$  = Pitzer's model parameters

$I$  = molality scale ionic strength, mol kg<sup>-1</sup>(H<sub>2</sub>O)

$N_p$  = Total number of measured point

$P$  = pressure, MPa

$T$  = temperature, K

### Lowercase

$a_{\text{CO}_2}$ ,  $a_{\text{H}_2\text{O}}$  = activity of dissolved CO<sub>2</sub> in the aqueous phase and H<sub>2</sub>O in CO<sub>2</sub>-rich phase, respectively

$a_i$  = parameters for calculating combined Pitzer interaction parameters

$b$  = constant in Pitzer's activity model,  $b = 1.2 \text{ kg}^{1/2} \text{ mol}^{-1/2}$

$k_{\text{H,CO}_2}^0$  = Henry's constant, bar mol<sup>-1</sup> kg

$m_a$ ,  $m_c$  = molality of dissolved anion and cation ions in the aqueous phase, mol kg<sup>-1</sup>

$m_{\text{CO}_2}$  = molality of CO<sub>2</sub> in the aqueous phase, mol kg<sup>-1</sup>

$m_{\text{CO}_2}^0$  = molality of CO<sub>2</sub> in the pure water, mol kg<sup>-1</sup>

$m_{\text{CO}_2,i}^{\text{calc}}$  = calculated molality of CO<sub>2</sub> by CO<sub>2</sub> solubility models, mol kg<sup>-1</sup>

$m_{\text{CO}_2,i}^{\text{exp}}$  = experimental CO<sub>2</sub> solubility taken from literature, mol kg<sup>-1</sup>

$m_{\text{salt}}$  = molality of salt species in aqueous solution

$q_i$  = parameters for calculating Pitzer ion-ion binary interaction parameters for the binary salt-H<sub>2</sub>O systems

$\bar{V}_{\text{CO}_2}$  = an empirical determined parameter in the proposed CO<sub>2</sub> solubility model, cm<sup>3</sup> mol<sup>-1</sup>

$\bar{V}_w$  = partial molar volume of water, cm<sup>3</sup> mol<sup>-1</sup>

$x_{\text{CO}_2}$ ,  $y_{\text{CO}_2}$  = mole fraction of CO<sub>2</sub> and H<sub>2</sub>O in the aqueous phase

### Greek

$\alpha_1$  = a constant for Pitzer's model,  $\alpha_1 = 2.0 \text{ kg}^{0.5} \text{ mol}^{-0.5}$

$\beta_{\text{ca}}^{(0)}$ ,  $\beta_{\text{ca}}^{(1)}$  = Pitzer ion-ion binary interaction parameters for Salt-H<sub>2</sub>O systems

$\gamma_{\text{CO}_2}$  = activity coefficient of dissolved CO<sub>2</sub> in the aqueous salt solutions

$\gamma_{\text{CO}_2}^0$  = activity coefficient of dissolved CO<sub>2</sub> in the pure water

$\lambda_{\text{nc}}$ ,  $\lambda_{\text{na}}$  = Pitzer interaction parameters between neutral species and ions

$\lambda_{\text{nn}}$ ,  $\mu_{\text{nn}}^{(g)}$ ,  $\mu_{\text{CO}_2}^{(g)}$ ,  $\mu_{\text{CO}_2}^{(aq)}$  = Pitzer interaction parameters for neutral species and the aqueous phase for a binary CO<sub>2</sub>-H<sub>2</sub>O system

$\mu_{\text{CO}_2}^{(g)}$ ,  $\mu_{\text{CO}_2}^{(aq)}$  = chemical potential of CO<sub>2</sub> in both the CO<sub>2</sub>-rich phase and the aqueous phase for a ternary CO<sub>2</sub>-salt-H<sub>2</sub>O system

$v^+$ ,  $v^-$  = stoichiometric number of cations and anions of a dissolved salt

$\xi_{\text{nca}}$ ,  $\mu_{\text{nna}}$ ,  $\mu_{\text{nnc}}$  = Pitzer triple interaction parameters between neutral species and ions

$\phi$  = osmotic coefficient

$\phi_{\text{CO}_2}$ ,  $\phi_{\text{H}_2\text{O}}$  = fugacity coefficient of CO<sub>2</sub> and H<sub>2</sub>O, computed by the modified RK EoS

$\phi_w^s$  = fugacity coefficient of pure H<sub>2</sub>O, computed by IAPWS-95 EoS

## Literature Cited

- Al-Anezi K, Hilal N. Scale formation in desalination plants: effect of carbon dioxide solubility. *Desalination*. 2007;204:385–402.
- Peker H, Srinivasan MP, Smith JM, McCoy BJ. Caffeine extraction rates from coffee beans with supercritical carbon dioxide. *AIChE J*. 1992;38:761–770.
- Benson SM, Cole DR. CO<sub>2</sub> sequestration in deep sedimentary formations. *Elements*. 2008;4:325–331.
- Pruess K. Enhanced geothermal systems (EGS) using CO<sub>2</sub> as working fluid—a novel approach for generating renewable energy with simultaneous sequestration of carbon. *Geothermics*. 2006;35:351–367.
- Dicharry RM, Perryman TL, Ronquille JD. Evaluation and design of a CO<sub>2</sub> miscible flood project-SACROC unit, Kelly-Snyder field. *J Pet Technol*. 1973;25:1309–1318.
- Videm K, Koren AM. Corrosion, passivity, and pitting of carbon steel in aqueous solutions of HCO<sub>3</sub>, CO<sub>2</sub>, and Cl. *Corrosion Sci*. 1993;49:746–754.
- Spycher N, Pruess K. A phase-partitioning model for CO<sub>2</sub>-brine mixtures at elevated temperatures and pressures: application to CO<sub>2</sub>-enhanced geothermal systems. *Transp Porous Media*. 2010;82:173–196.
- Springer RD, Wang Z, Anderko A, Wang P, Felmy AR. A thermodynamic model for predicting mineral reactivity in supercritical carbon dioxide: I. Phase behavior of carbon dioxide-water-chloride salt systems across the H<sub>2</sub>O-rich to the CO<sub>2</sub>-rich regions. *Chem Geol*. 2012;322–323:151–171.
- Mao S, Zhang D, Li Y, Liu N. An improved model for calculating CO<sub>2</sub> solubility in aqueous NaCl solutions and the application to CO<sub>2</sub>-H<sub>2</sub>O-NaCl fluid inclusions. *Chem Geol*. 2013;347:43–58.
- Zhao H, Fedkin MV, Dillmore RM, Lvov SN. Carbon dioxide solubility in aqueous solutions of sodium chloride at geological conditions: experimental results at 323.15, 373.15, 423.15 K and 150 bar and modeling up to 573.15 K and 2000 bar. *Geochim Cosmochim Acta*. 2015;149:165–189.
- Dresel PE, Rose AW. Chemistry and origin of oil and gas well brines in western pennsylvania. Open-file oil and gas report 10-01.0, Fourth Series. Harrisburg, Pennsylvania Geological Survey, 2010.
- McIntosh JC, Water LM, Martini AM. Extensive microbial modification of formation water geochemistry: case study from a midcontinent sedimentary basin, United States. *Geol Soc Am Bull*. 2004;116:743–759.
- Yan Y, Chen C-C. Thermodynamic modeling of CO<sub>2</sub> solubility in aqueous solutions of NaCl and Na<sub>2</sub>SO<sub>4</sub>. *J Supercrit Fluids*. 2010;55:623–634.
- Pérez-Salado Kamps Á, Meyer E, Rumpf B, Maurer G. Solubility of CO<sub>2</sub> in aqueous solutions of KCl and in aqueous solutions of K<sub>2</sub>CO<sub>3</sub>. *J Chem Eng Data*. 2007;52:817–832.
- Spycher N, Pruess K, Ennis-King J. CO<sub>2</sub>-H<sub>2</sub>O mixtures in the geological sequestration of CO<sub>2</sub>. I. Assessment and calculation of mutual solubilities from 12 to 100°C and up to 600 bar. *Geochim Cosmochim Acta*. 2003;67:3015–3031.
- Duan Z, Sun R. An improved model calculating CO<sub>2</sub> solubility in pure water and aqueous NaCl solutions from 273 to 533 K and from 0 to 2000 bar. *Chem Geol*. 2003;193:257–271.



17. Duan Z, Sun R, Zhu C, Chou I-M. An improved model for the calculation of CO<sub>2</sub> solubility in aqueous solutions containing Na<sup>+</sup>, K<sup>+</sup>, Ca<sup>2+</sup>, Mg<sup>2+</sup>, Cl<sup>-</sup>, and SO<sub>4</sub><sup>2-</sup>. *Mar Chem*. 2006;98:131–139.
18. Prausnitz JM, Tavares FW. Thermodynamics of fluid-phase equilibria for standard chemical engineering operations. *AIChE J*. 2004;50:739–761.
19. Ball FX, Fürst W, Renon H. An NRTL model for representation and prediction of deviation from ideality in electrolyte solutions compared to the models of Chen (1982) and Pitzer (1973). *AIChE J*. 1985;31:392–399.
20. Wagner W, Pruf A. The IAPWS formulation 1995 for the thermodynamic properties of ordinary water substance for general and scientific use. *J Phys Chem Ref Data*. 2002;31:387–535.
21. Akinfiev NN, Diamond LW. Thermodynamic model of aqueous CO<sub>2</sub>-H<sub>2</sub>O-NaCl solutions from –22 to 100 °C and from 0.1 to 100 MPa. *Fluid Phase Equilib*. 2010;295:104–124.
22. Prutton CF, Savage RL. The solubility of carbon dioxide in calcium chloride-water solutions at 75, 100, 120 and high pressures. *J Am Chem Soc*. 1945;67:1550–1554.
23. Onda K, Sada E, Kobayashi T, Kito S, Ito K. Salting-out parameters of gas solubility in aqueous salt solutions. *J Chem Eng Jpn*. 1970;3:18–24.
24. Malinin SD, Savelyeva NI. The solubility of CO<sub>2</sub> in NaCl and CaCl<sub>2</sub> solutions at 25, 50 and 75 °C under elevated CO<sub>2</sub> pressures. *Geochem Int*. 1972;9:410–418.
25. Malinin SD, Kurovskaya NA. Investigations of CO<sub>2</sub> solubility in a solution of chlorides at elevated temperatures and pressures of CO<sub>2</sub>. *Geochem Int*. 1975;12:199–201.
26. Yasunishi A, Yoshida F. Solubility of carbon dioxide in aqueous electrolyte solutions. *J Chem Eng Data*. 1979;24:11–14.
27. Liu Y, Hou M, Yang G, Han B. Solubility of CO<sub>2</sub> in aqueous solutions of NaCl, KCl, CaCl<sub>2</sub> and their mixed salts at different temperatures and pressures. *J Supercrit Fluids*. 2011;56:125–129.
28. Corti HR, Krenzer ME, De Pablo JJ, Prausnitz JM. Effect of a dissolved gas on the solubility of an electrolyte in aqueous solution. *Ind Eng Chem Res*. 1990;29:1043–1050.
29. Rumpf B, Maurer G. An experimental and theoretical investigation on the solubility of carbon dioxide in aqueous solutions of strong electrolytes. *Ber der Bunsengesellschaft für physikalische Chem*. 1993;97:85–97.
30. Bermejo MD, Martín A, Florusse LJ, Peters CJ, Cocero MJ. The influence of Na<sub>2</sub>SO<sub>4</sub> on the CO<sub>2</sub> solubility in water at high pressure. *Fluid Phase Equilib*. 2005;238:220–228.
31. Markham AE, Kobe KA. The solubility of carbon dioxide and nitrous oxide in aqueous salt solutions. *J Am Chem Soc*. 1941;63:449–454.
32. Gerecke J. Ein Beitrag zur Gaslöslichkeit in Elektrolytlösungen. Untersucht am Beispiel der Löslichkeit von H<sub>2</sub>, CO<sub>2</sub> und NH<sub>3</sub> in Wasser und wässrigen Salzlösungen, Ph.D. Dissertation, Technische Hochschule für Chemie Carl Schorlemmer - Leuna Merseburg, 1969.
33. Burmakina GV, Efanov LN, Shnet MA. CO<sub>2</sub> solubility in aqueous solutions of some electrolytes and sucrose. *Russ J Phys Chem*. 1982;56:705–707.
34. Kiepe J, Horstmann S, Fischer K, Gmehling J. Experimental determination and prediction of gas solubility data for CO<sub>2</sub> + H<sub>2</sub>O mixtures containing NaCl or KCl at temperatures between 313 and 393 K and pressures up to 10 MPa. *Ind Eng Chem Res*. 2002;41:4393–4398.
35. Setschenow J. Über die konstitution der salzlösungen auf grund ihres verhaltens zu kohlenensäure. *Ann de Chimie de Physique*. 1892;25:226–270.
36. Geffcken G. Beiträge zur Kenntnis der Löslichkeitsbeeinflussung. Ph.D. Dissertation, Leipzig University, 1904.
37. Findley A, Shen B. CLVI.—The influence of colloids and fine suspensions on the solubility of gases in water. Part II. Solubility of carbon dioxide and of hydrogen. *J Chem Soc Trans*. 1912;101:1459–1468.
38. Kobe KA, Williams JS. Confining liquids for gas analysis: solubility of carbon dioxide in salt solutions. *Ind Eng Chem*. 1935;7:37–38.
39. Tong D, Martin Trusler JP, Vega-Maza D. Solubility of CO<sub>2</sub> in aqueous solutions of CaCl<sub>2</sub> or MgCl<sub>2</sub> and in a synthetic formation brine at temperatures up to 423 K and pressures up to 40 MPa. *J Chem Eng Data*. 2013;58:2116–2124.
40. Scharlin P, International Union of Pure and Applied Chemistry. *Carbon Dioxide in Water and Aqueous Electrolyte Solutions, Solubility Data Series*, Vol 62. Oxford, UK: Oxford University Press, 1996.
41. Li YH, Tsui TF. The solubility of CO<sub>2</sub> in water and sea water. *J Geophys Res*. 1971;76:4203–4207.
42. Buch K, Harvey HW, Wattenberg H, Gripenberg S. Über dem Kohlensäuresystem im Meerwasser, Rapports et procès-verbaux des réunions. *Conseil Permanent International Pour l'Exploration de la Mer*. 1932;79:1–70.
43. Samoilov OY. A new approach to the study of hydration ion in aqueous solutions. *Discuss Faraday Soc*. 1957;24:141–146.
44. Collins KD. Charge density-dependent strength of hydration and biological structure. *Biophys J*. 1997;72:65–76.
45. Marcus Y. Ionic radii in aqueous solutions. *Chem Rev*. 1988;88:1475–1498.
46. Takenouchi S, Kennedy GC. The binary system H<sub>2</sub>O-CO<sub>2</sub> at high temperature and pressures. *Am J Sci*. 1964;262:1055–1074.
47. Tödheide K, Franck EU. Das Zweiphasengebiet und die kritische Kurve im system kohlendioxid-wasser bis zu drucken von 3500 bar. *Z Phys Chem (N F)*. 1963;37:387–401.
48. Mather AE, Franck EU. Phase equilibria in the system carbon dioxide-water at elevated pressures. *J Phys Chem*. 1992;96:6–8.
49. Wiebe R, Gaddy VL. Vapor phase composition of carbon dioxide-water mixtures at various temperatures and at pressures to 700 atmospheres. *J Am Chem Soc*. 1941;63:475–477.
50. King MB, Mubarak A, Kim JD, Bott TR. The mutual solubilities of water with supercritical and liquid carbon dioxide. *J Supercrit Fluids*. 1992;5:296–302.
51. Rowland D, Königsberger E, Hefter G, May PM. Aqueous electrolyte solution modelling: some limitations of the Pitzer equations. *Appl Geochem*. 2015;55:170–183.
52. Setschenow J. Über die konstitution der salzlösungen auf grund ihres verhaltens zu kohlenensäure. *Z Phys Chem*. 1889;4:117–128.
53. Zhao H, Robert DM, Douglas A, Yee S, Serguei NL. Measurement and modeling of CO<sub>2</sub> solubility in natural and synthetic formation brines. *Environ Sci Technol*. 2015;49:1972–1980.
54. Pitzer KS. *Activity Coefficients in Electrolyte Solutions*, 2nd ed. Boca Raton: CRC Press, 1991.

## Appendix : Additional Model Equations

The Pitzer equations for the activity coefficient of dissolved CO<sub>2</sub> and the osmotic coefficient of water are shown below as Eqs. A1 and A2, respectively<sup>54</sup>

$$\ln \gamma_{\text{CO}_2} = 2m_{\text{CO}_2} \lambda_{\text{nn}} + 3m_{\text{CO}_2}^2 \mu_{\text{nnn}} + 2\lambda_{\text{nc}} m_{\text{c}} + 2\lambda_{\text{na}} m_{\text{a}} + m_{\text{a}} m_{\text{c}} \zeta_{\text{nca}} + 6m_{\text{CO}_2} m_{\text{c}} \mu_{\text{nnc}} + 6m_{\text{CO}_2} m_{\text{a}} \mu_{\text{nna}} \quad (\text{A1})$$

$$\phi - 1 = \frac{2}{m_{\text{a}} + m_{\text{c}} + m_{\text{CO}_2}} \left\{ -A^\phi \frac{I^{1.5}}{I + bI^{0.5}} + m_{\text{a}} m_{\text{c}} [\beta_{\text{ca}}^{(0)} + \beta_{\text{ca}}^{(1)} \exp(-\alpha_1 I^{0.5})] + (m_{\text{a}} |z_{\text{a}}| + m_{\text{c}} |z_{\text{c}}|) C_{\text{ca}} \right\} + \frac{1}{2} m_{\text{CO}_2}^2 \lambda_{\text{nn}} + m_{\text{CO}_2}^3 \mu_{\text{nnn}} + m_{\text{CO}_2} m_{\text{c}} \lambda_{\text{nc}} + 3m_{\text{CO}_2}^2 m_{\text{c}} \mu_{\text{nnc}} + m_{\text{CO}_2} m_{\text{a}} \lambda_{\text{na}} + 3m_{\text{CO}_2}^2 m_{\text{a}} \mu_{\text{nna}} + m_{\text{CO}_2} m_{\text{a}} m_{\text{c}} \zeta_{\text{nca}} \quad (\text{A2})$$

In these equations,  $m_{\text{CO}_2}$  is the molality of CO<sub>2</sub>;  $m_{\text{a}}$  and  $m_{\text{c}}$  are, respectively, the molality of anions and cations in the aqueous phase. In Eq. 2,  $C_{\text{ca}} = 0.5 C_{\text{ca}}^\phi / |z_{\text{c}} z_{\text{a}}|^{0.5}$ ,  $A^\phi$  is the Debye-Hückel slope for the osmotic coefficient, and  $b = 1.2 \text{ kg}^{1/2} \text{ mol}^{-1/2}$ ,  $\alpha_1 = 2.0 \text{ kg}^{1/2} \text{ mol}^{-1/2}$ .  $I$  is the ionic strength based on the molal concentration scale. The empirical equations for calculating the Pitzer binary ion-ion interaction parameters ( $\beta_{\text{ca}}^{(0)}$ ,  $\beta_{\text{ca}}^{(1)}$ , and  $C_{\text{ca}}$ ) were taken from literature and summarized in the Appendix. The Pitzer pure CO<sub>2</sub> interaction parameters ( $\lambda_{\text{nn}}$  and  $\mu_{\text{nnn}}$ ) in the temperature range 273.15–573.15 K can be found in Zhao et al.<sup>10</sup>

Manuscript received Jan. 2, 2015, and revision received Mar. 31, 2015.